

Giant Nernst and Hall Effects in Chiral Superconductors due to Berry Phase Fluctuations

Hiroaki Sumiyoshi¹ and Satoshi Fujimoto^{1,2}

¹*Department of Physics, Kyoto University, Kyoto 606-8502, Japan and*

²*Department of Materials Engineering Science, Osaka University, Toyonaka 560-8531, Japan*

(Dated: July 24, 2014)

We consider the Nernst and Hall effects in fluctuation regime of chiral superconductors above transition temperatures, that are raised not by conventional Lorentz force, but by asymmetric scattering due to fluctuations of the Berry phase of the Bogoliubov-de Gennes Hamiltonian. It is found that these effects can be more significant than conventional ones for cleaner samples, exhibiting qualitatively distinct behaviors. The results provide systematic and comprehensive understanding for recent experimental observations of the Nernst effect in a clean URu₂Si₂ sample, which is suggested to be a chiral superconductor.

PACS numbers: 74.25.fc 74.20.-z 74.62.-c 74.70.Tx

In a certain class of superconductors, fluctuations toward ordered states above transition temperatures give rise to dramatic effects on many-body electron states. It is known that a powerful probe for such phenomena is the Nernst effect. For instance, giant Nernst signals have been observed in near and above transition temperatures T_c of cuprate high- T_c superconductors [1] and dirty superconducting thin films [2]. In normal metals, the Nernst signal is generally weak owing to the Sondheimer cancelation [3] and then, these unexpected experimental observations inspired succeeding extensive studies, leading to various theoretical proposals such as scenarios based on short-lived Cooper pairs [4], Josephson electromotive force due to the vortex motion [5], and strong coupling with antiferromagnetic fluctuations [6].

In this letter, we propose an unconventional mechanism for the giant Nernst effect above T_c in *chiral superconductors*, which has not been discussed so far. In chiral superconductors, time-reversal symmetry (TRS) is spontaneously broken, and total angular momentum carried by Cooper pairs is nonzero. The “chirality” of this superconducting state is characterized by the Berry phase of the Bogoliubov-de Gennes mean-field Hamiltonian, which is an Aharonov-Bohm (AB) phase whose adiabatic parameters are the wave number [7]. In the superconducting phase below T_c , the intrinsic magnetic field induced by it causes exotic transverse transport phenomena under zero external magnetic field, such as the Kerr effect [8, 9], which was observed in Sr₂RuO₄ [10], and the anomalous thermal Hall effect, which was theoretically predicted [11–13]. It is natural to expect that also in the superconducting fluctuation regime above T_c , characteristic transverse transport phenomena can be induced by fluctuations of the chirality or the Berry phase. We investigate this possibility, and clarify a novel mechanism of the giant Nernst and Hall effects above and near T_c , caused by Berry phase fluctuations. In this scenario, quasiparticles are scattered asymmetrically by fluctuating Cooper pairs with angular momentum, even without Lorentz force, and then, such effects can be regarded as an analog of the skew scattering process of the anomalous

Hall effect, which is caused by a spin-orbit coupling involving impurity scattering [14], but a major difference is that the scattering kernels are dynamical in this case.

There are several candidate systems for chiral superconductors, e.g. Sr₂RuO₄, URu₂Si₂, doped graphene/silicene, SrPtAs, and Na_xCoO₂ · y H₂O [15–23]. Among them, the heavy-electron superconductor URu₂Si₂, whose pairing symmetry is suggested to be chiral $d_{zx} \pm id_{zy}$ [16–18], is one of the most promising one for the realization of the above-mentioned mechanism, because, for this system, strong superconducting fluctuation effects have been experimentally observed, which may be attributed to small energy scale raised by heavy effective mass and the reconstruction of electronic structures in the so-called hidden order phase [24]. Thus, in this letter, we mainly focus on this system, though our theory is also applicable to other chiral superconductors with minor modifications.

Our approach is based on microscopic model calculations utilizing linear response theory for the Nernst and Hall effects. The Hall conductivity is given by the Kubo formula: $\sigma_{\alpha\beta} = S_{\alpha\beta}^R(\omega)/(-i\omega)|_{\omega \rightarrow 0}$, where $S_{\alpha\beta}^R(\omega)$ is the retarded current-current correlation function. On the other hand, the case of the Nernst effect is more involved. As pointed out by previous studies, one needs to take account of contributions from magnetization \mathbf{M} in addition to those from the Kubo formula [25–28]. Then, the Nernst conductivity (Peltier coefficient) is,

$$\begin{aligned}\alpha_{\alpha\beta} &= \alpha_{\alpha\beta}^{Kubo} + \alpha_{\alpha\beta}^{mag}, \\ \alpha_{\alpha\beta}^{mag} &= \epsilon_{\alpha\beta\gamma} M^\gamma / T.\end{aligned}\quad (1)$$

Here, $\alpha_{\alpha\beta}^{Kubo}$ is the Kubo term given by the heat-current-charge-current correlation function. We apply diagram techniques to calculate these transport coefficients.

Model — The Hamiltonian with which we start is an effective model for the superconducting state of URu₂Si₂ which belongs to E_g representation of the point group

D_{4h} [29]:

$$H = \sum_{\mathbf{k}\sigma} \xi_{\mathbf{k}} c_{\mathbf{k}\sigma}^\dagger c_{\mathbf{k}\sigma} - g \sum_{\mathbf{k}, \mathbf{k}', \mathbf{q}} V(\mathbf{k}, \mathbf{k}') c_{\mathbf{k}+\mathbf{q}/2\uparrow}^\dagger c_{-\mathbf{k}+\mathbf{q}/2\downarrow}^\dagger c_{-\mathbf{k}'+\mathbf{q}/2\downarrow} c_{\mathbf{k}'+\mathbf{q}/2\uparrow}, \quad (2)$$

where, for simplicity, we take a spherical Fermi surface, $\xi_{\mathbf{k}} = \mathbf{k}^2/2m - \mu$, and the effective attractive interaction is given by $V(\mathbf{k}, \mathbf{k}') = 15(k_z k_x k'_z k'_x + k_z k_y k'_z k'_y)/k_F^4$. It is the model for the chiral $d_{zx} \pm id_{zy}$ superconductor URu₂Si₂. In the chiral superconducting phase, TRS is spontaneously broken and the gap function takes the form $\Delta(\mathbf{k}) \propto k_z(k_x + ik_y)$ (or $k_z(k_x - ik_y)$), which is caused by an effective attractive interaction, $V^+(\mathbf{k}, \mathbf{k}') = \phi(\mathbf{k})\phi^\dagger(\mathbf{k}')$ (or $V^-(\mathbf{k}, \mathbf{k}') = \phi^\dagger(\mathbf{k})\phi(\mathbf{k}')$), where the pairing symmetry function reads $\phi(\mathbf{k}) = \sqrt{15/2}k_z(k_x + ik_y)/k_F^2$. Note that $V(\mathbf{k}, \mathbf{k}') = V^+(\mathbf{k}, \mathbf{k}') + V^-(\mathbf{k}, \mathbf{k}')$. The channel $V^{+(-)}$ is associated with the chirality $C = +1$ (-1), and each channel breaks TRS. However, we concentrate on transport phenomena above T_c , in fluctuation regime, where two channels are degenerate, and therefore TRS is *not* spontaneously broken.

Nernst and Hall Effects — Generally, to induce transverse transport phenomena such as the Nernst and Hall effects, it is necessary to break TRS. In fluctuation regime above T_c , TRS is not spontaneously broken, and then a magnetic field is necessary unlike spontaneous Kerr and thermal Hall effects in the chiral superconducting phases [8–13]. Due to a magnetic field, the Lorentz force on quasiparticles and fluctuating Cooper pairs is generated and causes conventional transverse transport phenomena [30]. In addition, in the case of chiral superconductors, the magnetic field also causes “polarization” of chirality due to a magnetic field-chirality (MC) coupling; i.e. the difference in the weights of two superconducting fluctuation channels is induced. The chirality-polarized superconducting fluctuations give rise to asymmetric scattering of electrons resulting in the anomalous Nernst and Hall effects (ANE and AHE) without Lorentz force, which are the main subjects of this letter (See Eqs.(4), (5), and (8) below, which constitute the main results).

First, we discuss the chirality polarization by evaluating the superconducting fluctuation propagator. Under a uniform magnetic field $\mathbf{H} = (0, 0, H)$, the fluctuation propagators of chiral $d_{zx} \pm id_{zy}$ -channels (correspond to $C = \pm 1$, respectively) is given by [31]:

$$\begin{aligned} \tilde{L}_C^{-1}(\mathbf{x}, \mathbf{y}, \omega_q; H) &= -\frac{\delta(\mathbf{x} - \mathbf{y})}{g} + \tilde{\Pi}_C(\mathbf{x}, \mathbf{y}, \omega_q; H), \\ \tilde{\Pi}_C(\mathbf{x}, \mathbf{y}, \omega_q; H) &= e^{-i2e\Phi(\mathbf{x}, \mathbf{y})} \\ &\times \left[\Pi(\mathbf{x} - \mathbf{y}, \omega_q; H) - C \frac{5eH}{4k_F^2} \Pi'(\mathbf{x} - \mathbf{y}, \omega_q; H) \right], \quad (3) \end{aligned}$$

where Π and Π' are “core” bare particle-particle susceptibilities (BPSs) of $d_{zx} \pm id_{zy}$ - and p_z -wave channels,

respectively, which preserve translation, gauge, and c -axis rotation invariances, ω_q is the bosonic Matsubara frequency, and the AB-phase, $\Phi(\mathbf{x}, \mathbf{y}) = \int_{\mathbf{x}}^{\mathbf{y}} \mathbf{A}(\mathbf{r}) d\mathbf{r}$, is defined as an integral of the vector potential along a straight line. Here we used the fact that the one-particle Green function in a magnetic field is given by $\tilde{G}(\mathbf{x}, \mathbf{y}, \varepsilon_n; H) = e^{-ie\Phi(\mathbf{x}, \mathbf{y})} G_{core}(\mathbf{x} - \mathbf{y}, \varepsilon_n; H)$, where G_{core} is the core Green function, which has translation, gauge, and c -axis rotation invariances [32, 33]. We note that this expression (3) is applicable to arbitrary magnitude of magnetic fields and for any gauge conditions. The remarkable point is the existence of the chirality-dependent term, $-C(5eH/4k_F^2)\Pi'$, which changes the amplitude of the BPS, reflecting the polarization mechanism due to the MC-coupling. The MC-coupling raises (lowers) the transition temperature of the $C = -1$ ($+1$) state, which has orbital magnetic moment parallel (antiparallel) to the c -axis, in contrast to the AB-phase, which reflects the orbital depairing effect, and always lowers the transition temperature [34]. Moreover, the MC-coupling induces paramagnetism discussed later.

Using the fluctuation propagator, Eq. (3), we calculate the Nernst and Hall conductivities. Note that up to the linear order in H , we can systematically separate whole contributions into two parts: one corresponding to the conventional contribution due to Lorentz force on quasiparticles and fluctuating Cooper pairs, and the other one associated with the ANE and AHE caused by the Berry-phase fluctuation mechanism. As will be shown below, the latter contribution dominates over the former one for clean samples. Thus, we focus on the latter in the following. The detail of the calculation based on diagrammatic techniques is presented in the Supplemental Material [31]. We sketch briefly a basic idea of the derivation for the Nernst and Hall conductivities. It is found that the three diagrams which give leading-order contributions in conventional theories, i.e. the Aslamazov-Larkin (AL), Maki-Thompson (MT), and density-of-states (DOS) diagrams (upper panel in Fig. 1) [30], do not contribute in this case, and generally, all contributions from diagrams belonging to the classes of the lower panel in Fig. 1 are zero [31]. The lowest order diagrams which do not belong to these classes and give nonzero contributions are depicted in Fig. 2. In these diagrams, inelastic scattering processes due to electron-electron interaction represented by a renormalized four-point vertex, $W(\mathbf{k}, \omega_k)$ (double line), are included. To carry out calculations explicitly, we postulate a simple model: $W(\mathbf{k}, \omega_k) = W_0/(1 + |\omega_k|/\Gamma)$, i.e. an interaction mediated via a short-range antiferromagnetic spin fluctuation, where W_0 is a constant and Γ is the energy scale of spin fluctuations. In fact, for URu₂Si₂, a short-range antiferromagnetic spin fluctuation exists in the hidden order phase as clarified by inelastic neutron scattering measurements [35, 36]. Thus, the above assumption for $W(\mathbf{k}, \omega_k)$ is legitimate. However, we stress that our final results are qualitatively not changed by specific form of $W(\mathbf{k}, \omega_k)$, as will be discussed later.

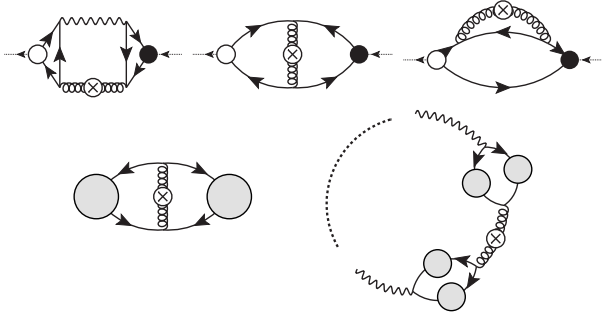


FIG. 1: *Upper panel*: AL, MT, and DOS diagrams. The AL and DOS diagrams have the mirror image counterparts. Wavy lines and curly lines with crossed circles represent the fluctuation propagator in zero magnetic field, L , and the chirality-polarized one, \tilde{L}'_C , respectively, where their definitions are given in [31]. Solid lines with arrows are the one-particle Green functions. Open circles represent electric current vertex, and bullets represent energy current vertex (electric current vertex), for α_{xy} (σ_{xy}). *Lower panel*: Diagrams in which the information of the chirality disappears, resulting in vanishing contributions to the Nernst or Hall effects. Shaded circles represent any diagrams without fluctuation propagators and the two current vertices are inserted into any propagators.

Then, we obtain the Kubo terms of the Nernst and Hall conductivities in clean limit, near T_c , and in the linear order of H [31]:

$$\frac{\alpha_{xy}^{Kubo}{}_{chiral}}{H} = \frac{f\left(\frac{2\pi T}{\Gamma}\right)}{2304} \frac{\tau^2 e^2 W_0 v_F^4 \Lambda}{\xi^4 g k_F^2 T^2} \left(1 - \frac{3\pi}{4} \frac{\sqrt{\varepsilon}}{\xi \Lambda}\right), \quad (4)$$

$$\frac{\sigma_{xy}{}_{chiral}}{H} = \frac{5f\left(\frac{2\pi T}{\Gamma}\right)}{1152} \frac{\tau^2 e^3 W_0 v_F^3 \Lambda}{\xi^4 g k_F^3 T} \left(1 - \frac{3\pi}{4} \frac{\sqrt{\varepsilon}}{\xi \Lambda}\right). \quad (5)$$

Here, $\varepsilon = \log T/T_c$, v_F is the Fermi velocity, $\xi = \sqrt{-\psi''(1/2)/6(v_F/4\pi T)}$ is the coherence length, ψ is the digamma function, τ is the electron scattering time due to impurities and electron-electron scattering, Λ is the cutoff of the momentum of superconducting fluctuation propagator, which is the same order as $1/\xi$, and $f(2\pi T/\Gamma)$ is a dimensionless function, whose definition and numerical estimations are given in [31].

Now, we discuss the magnetization contribution in Eq.(1). The magnetization due to chirality-polarized superconducting fluctuations is of interest not only because of its contribution to the Nernst effect, but also because of its unique magnetic property; i.e. the polarization of chiral superconducting fluctuation channels causes paramagnetism in contrast to diamagnetism due to fluctuating Meissner currents observed in general superconductors [30]. The calculation is performed with the free energy of chiral superconductors above T_c :

$$F[H] = T \sum_{\omega_q, C=\pm 1} \text{Tr} \ln(-\hat{\tilde{L}}_C^{-1}(\omega_q; H)), \quad (6)$$

where $\hat{\tilde{L}}_C^{-1}(\omega_q; H)$ is the matrix whose indices are spatial coordinates, \mathbf{x} and \mathbf{y} , and matrix elements are

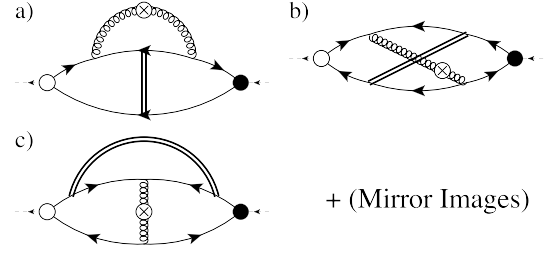


FIG. 2: Diagrams which contribute to the ANE and AHE raised by Berry-phase fluctuation mechanism. The double lines represent the renormalized four-point vertex, $W(\mathbf{k}, \omega_k)$ due to electron-electron interaction.

$\tilde{L}_C^{-1}(\mathbf{x}, \mathbf{y}, \omega_q; H)$, Eq. (3). From this free energy, we obtain the magnetic susceptibility $\chi = \chi_{dia} + \chi_{chiral}$ with

$$\chi_{chiral} = \frac{25e^2 T}{64\pi k_F^4 \xi^3 (N(0)g)^2 \varepsilon^{1/2}} > 0, \quad (7)$$

where χ_{dia} is the diamagnetic term due to fluctuating Meissner currents observed in general superconductors [30, 37], and χ_{chiral} is the paramagnetism term mentioned above [31]. Then, the magnetization current contribution inherent in chiral superconductors is

$$\frac{\alpha_{xy}^{mag}{}_{chiral}}{H} = \frac{\chi_{chiral}}{T} = \frac{25e^2}{64\pi k_F^4 \xi^3 (N(0)g)^2 \varepsilon^{1/2}}. \quad (8)$$

The total Nernst conductivity due to Berry-phase fluctuations is given by sum of Eqs. (4) and (8), which constitute our main results.

Discussions — We now discuss several important features of Eqs. (4) and (8). The critical behavior of the magnetization current contribution, (8), given by $\propto (T - T_c)^{-1/2}$, is the same as that of the AL term of the Nernst conductivity, which is also obtained from a time-dependent Ginzburg-Landau (TDGL) equation [4, 38]. On the other hand, the critical behavior of the Kubo contribution, (4), is less singular, $\propto (const. - \sqrt{T - T_c})$. However, we note that the dependence on scattering time τ of Eq. (4), which is proportional to τ^2 , is quite distinct from any conventional fluctuation-induced corrections to the Nernst coefficient previously studied so far. For instance, there is no τ -dependence in the contribution to α_{xy} that obtained by dynamics of boson fields (i.e. fields of Cooper pairs), such as the scenarios of short-lived Cooper pairs (i.e. the conventional AL term) [4] and the vortex motion [5]. This is simply because that dynamics of bosons do not involve quasiparticle scattering time. Also, it is known that contributions from electron dynamics influenced by the fluctuation boson field, including the MT and DOS terms, do not yield τ -dependent α_{xy} [39, 40]. Thus, for sufficiently clean samples with large τ , the Kubo term $\alpha_{xy}^{Kubo}{}_{chiral}$ of the Berry-phase fluctuation mechanism significantly dominates over contributions from the AL, MT, and DOS terms of the Nernst

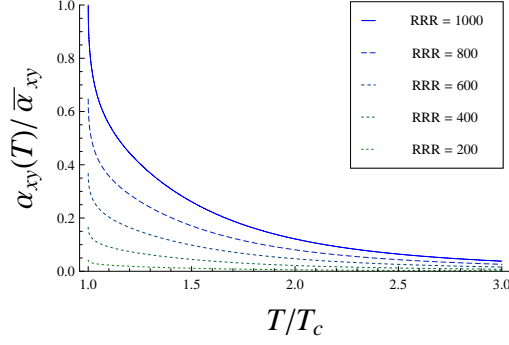


FIG. 3: (Color online). α_{xy} raised by the Berry-phase fluctuation mechanism versus T/T_c for several values of RRR. The magnitudes of α_{xy} are normalized by the value of the most clean one at T_c , $\bar{\alpha}_{xy} := \alpha_{xy}(T_c; \text{RRR} = 1000)$. We used the material parameters of URu₂Si₂ [41].

conductivity raised by conventional Lorentz force. Furthermore, because of the τ -dependence, the Kubo term α_{xy}^{Kubo} is also much more enhanced than the magnetization term (8) for cleaner samples. Thus, the leading term of the Nernst conductivity for clean chiral superconductors is given by α_{xy}^{Kubo} . The unusual τ -dependence of α_{xy}^{Kubo} combined with an increasing behavior for T approaching to T_c , as shown in Eq. (4) characterizes the distinct feature of the Berry-phase fluctuation mechanism. In Fig. 3, we plot typical temperature dependences of Eq. (4) for several values of τ parametrizing the residual resistivity ratio (RRR) of samples. Here, we used material parameters of URu₂Si₂ [41], and the calculation was achieved by using an approximation scheme explained in [31]. As discussed above, α_{xy} exhibits remarkably strong enhancement in the vicinity of T_c for cleaner systems. It is an intriguing feature issue to test our theory for real materials. On the other hand, the Hall conductivity, Eq. (5), has the same characteristic τ -dependence, $\propto \tau^2$, as α_{xy}^{Kubo} , and, moreover, is nonzero even when the electronic band is particle-hole symmetric. This point is quite different from conventional contributions derived from TDGL equation or, equivalently, the AL term, which requires particle-hole band asymmetry: $\partial T_c / \partial \mu \neq 0$ (equivalently $\partial N(0) / \partial \mu \neq 0$ or $\partial g / \partial \mu \neq 0$) [42]. However, it would be rather more difficult to detect the Hall effect than the Nernst effect, because normal Hall currents of conventional Fermi-liquid quasiparticles dominate for charge transport.

These τ -dependences of the Peltier and Hall coefficients for the Berry-phase fluctuation mechanism, $\alpha_{xy}, \sigma_{xy} \propto \tau^2$, can be also understood from the following phenomenological argument. In our mechanism, the Nernst and Hall effects are caused by the asymmetric (or skew) scattering processes of quasiparticles due to chiral superconducting fluctuation. Contributions from such asymmetric scattering processes to off-diagonal compo-

nents of transport tensors, e.g. α_{xy}, σ_{xy} , spin Hall coefficient, and so on, are proportional to τ^2 / τ_{skew} , where τ is the scattering time due to whole scattering processes and τ_{skew} is that due to asymmetric scattering processes. This relationship can be derived phenomenologically by using the Boltzmann equation with the quasiparticle scattering rate that has the asymmetric part [14, 43]. In this case, the scattering kernels which cause the skew scattering are not impurities but chiral superconducting fluctuations. Therefore, τ_{skew} is independent of the purity of the system, and then $\alpha_{xy}, \sigma_{xy} \propto \tau^2$, in contrast to the usual AHE raised by skew-scattering due to impurities, for which $\tau_{skew} \propto \tau$.

Finally, we discuss to what extent our results depend on the form of the effective potential, $W(\mathbf{k}, \omega_k)$, the spatial dimensionality and pairing symmetry of chiral superconducting states. We examined that the τ -dependence of Eqs. (4) and (5) in clean limit is not changed by these factors. However, the magnitude of the transport coefficients depends on the specific form of $W(\mathbf{k}, \omega_k)$: the contributions are decreased as the momentum-dependence of the interaction is stronger. Also, the most singular parts of T -dependence of (4) and (5) are not much affected by the specific form of $W(\mathbf{k}, \omega_k)$, though the dimensionality may change it. We present the precise argument in [31].

Implications for Experiments — We discuss the implication of our results for experiments. The Nernst effect is observed by measuring the Nernst coefficient which is the ratio of an induced transverse electric field ($\mathbf{E} \parallel \hat{\mathbf{y}}$) to product of temperature gradient ($\nabla T \parallel \hat{\mathbf{x}}$) and an applied magnetic field ($\mathbf{H} \parallel \hat{\mathbf{z}}$): $\nu^{NE} = E_y / (-\nabla_x T) H = (\alpha_{xy} \sigma_{xx} - \alpha_{xx} \sigma_{xy}) / (\sigma_{xx}^2 + \sigma_{xy}^2) H$. Usually, the longitudinal conductivity is dominated by contributions from conventional quasiparticles of the Fermi liquid rather than that from the superconducting fluctuations, i.e. $\sigma_{xx}^n \gg \sigma_{xx}^{Fluc}$. Also, for URu₂Si₂, as verified experimentally, $\alpha_{xy} / \sigma_{xx} \gg S \tan \Theta_H$, where S is the Seebeck constant and Θ_H is the Hall angle [44]. Thus, the Nernst coefficient is approximated as $\nu^{NE} \approx \nu^{NE n} + \nu^{NE Fluc}$, where $\nu^{NE n}$ is the usual Fermi liquid contribution, and $\nu^{NE Fluc} = \alpha_{xy}^{Fluc} / \sigma_{xx}^n H$ with α_{xy}^{Fluc} the superconducting fluctuation term (note that what appears in the denominator is not σ_{xx}^{Fluc} but σ_{xx}^n). As mentioned above, α_{xy} due to conventional fluctuation mechanism does not depend on τ , and thus, $\nu^{NE Fluc} \propto \tau^{-1}$ for non-chiral superconductors, which implies that this effect is suppressed for cleaner samples with larger τ [45]. In contrast, the Berry-phase fluctuation mechanism gives $\nu_{BPF}^{NE Fluc} \propto \tau^1$ and, therefore, it is more enhanced for cleaner samples.

Recently, the measurement of the Nernst effect for clean samples of URu₂Si₂ with different values of RRRs was carried out by Kyoto group [44]. They found that the Nernst coefficient above T_c is strongly enhanced in cleaner samples. Therefore, our scenario provides a promising explanation for this anomalous behavior.

Summary — We elucidate the unconventional mechanism of the Nernst and Hall effects raised by Berry-phase fluctuations above T_c in chiral superconductors. We pro-

pose that our theory can be tested for URu₂Si₂, which is believed to be a chiral $d + id$ superconductor with strong superconducting fluctuations above T_c .

We thank T. Yamashita, S. Tonegawa, Y. Tsuruhara, Y. Shimoyama, T. Shibauchi, and Y. Matsuda, for providing experimental data which give us motivation of this study, and A. Shitade, K. Shiozaki, T. Nomoto, and R.

Ikeda for helpful discussions. This work was supported by the Grant-in-Aids for Scientific Research from MEXT of Japan [Grants No. 23540406, No. 25220711, and No. 25103714 (KAKENHI on Innovative Areas Topological Quantum Phenomena)]. H. S. is supported by a JSPS Fellowship for Young Scientists.

-
- [1] Z. Xu, N. Ong, Y. Wang, T. Kakeshita, and S. Uchida, *Nature* **406**, 486 (2000).
 - [2] A. Pourret, H. Aubin, J. Lesueur, C. A. Marrache-Kikuchi, L. Bergé, L. Dumoulin, and K. Behnia, *Nature Phys.* **2**, 683 (2006).
 - [3] K. Behnia, *J. Phys.: Condens. Matter* **21**, 113101 (2009).
 - [4] I. Ussishkin, S. Sondhi, and D. Huse, *Phys. Rev. Lett.* **89**, 287001 (2002).
 - [5] Y. Wang, Z. A. Xu, T. Kakeshita, S. Uchida, S. Ono, Y. Ando, and N. P. Ong, *Phys. Rev. B* **64**, 224519 (2001).
 - [6] H. Kontani, *Phys. Rev. Lett.* **89**, 237003 (2002).
 - [7] G. Volovik, *The Universe in a Helium Droplet*, International Series of Monographs on Physics (OUP Oxford, 2009).
 - [8] A. Furusaki, M. Matsumoto, and M. Sigrist, *Phys. Rev. B* **64**, 054514 (2001).
 - [9] R. Roy and C. Kallin, *Phys. Rev. B* **77**, 174513 (2008).
 - [10] J. Xia, Y. Maeno, P. T. Beyersdorf, M. M. Fejer, and A. Kapitulnik, *Phys. Rev. Lett.* **97**, 167002 (2006).
 - [11] N. Read and D. Green, *Phys. Rev. B* **61**, 10267 (2000).
 - [12] K. Nomura, S. Ryu, A. Furusaki, and N. Nagaosa, *Phys. Rev. Lett.* **108**, 026802 (2012).
 - [13] H. Sumiyoshi and S. Fujimoto, *J. Phys. Soc. Jpn.* **82**, 023602 (2013).
 - [14] N. Nagaosa, J. Sinova, S. Onoda, A. H. MacDonald, and N. P. Ong, *Rev. Mod. Phys.* **82**, 1539 (2010).
 - [15] A. P. Mackenzie and Y. Maeno, *Rev. Mod. Phys.* **75**, 657 (2003).
 - [16] Y. Kasahara, T. Iwasawa, H. Shishido, T. Shibauchi, K. Behnia, Y. Haga, T. D. Matsuda, Y. Onuki, M. Sigrist, and Y. Matsuda, *Phys. Rev. Lett.* **99**, 116402 (2007).
 - [17] Y. Kasahara, H. Shishido, T. Shibauchi, Y. Haga, T. D. Matsuda, Y. Onuki, and Y. Matsuda, *New J. Phys.* **11**, 055061 (2009).
 - [18] K. Yano, T. Sakakibara, T. Tayama, M. Yokoyama, H. Amitsuka, Y. Homma, P. Miranović, M. Ichioka, Y. Tsutsumi, and K. Machida, *Phys. Rev. Lett.* **100**, 017004 (2008).
 - [19] R. Nandkishore, L. S. Levitov, and A. V. Chubukov, *Nature Phys.* **8**, 158 (2012).
 - [20] F. Liu, C.-C. Liu, K. Wu, F. Yang, and Y. Yao, *Phys. Rev. Lett.* **111**, 066804 (2013).
 - [21] P. K. Biswas, H. Luetkens, T. Neupert, T. Stürzer, C. Baines, G. Pascua, A. P. Schnyder, M. H. Fischer, J. Goryo, M. R. Lees, et al., *Phys. Rev. B* **87**, 180503 (2013).
 - [22] Fischer, Mark H., Neupert, Titus, Platt, Christian, Schnyder, Andreas P., Hanke, Werner, Goryo, Jun, Thomale, Ronny, and Sigrist, Manfred, *Phys. Rev. B* **89**, 020509 (2014).
 - [23] M. L. Kiesel, C. Platt, W. Hanke, and R. Thomale, *Phys. Rev. Lett.* **111**, 097001 (2013).
 - [24] R. Okazaki, Y. Kasahara, H. Shishido, M. Konczykowski, K. Behnia, Y. Haga, T. D. Matsuda, Y. Onuki, T. Shibauchi, and Y. Matsuda, *Phys. Rev. Lett.* **100**, 037004 (2008).
 - [25] J. M. Luttinger, *Phys. Rev.* **135**, A1505 (1964).
 - [26] Yu. N. Obraztsov, *Sov. Phys. Solid State* **6**, 331 (1964); **7**, 455 (1965).
 - [27] L. Smrcka and P. Streda, *J. Phys. C* **10**, 2153 (1977).
 - [28] N. R. Cooper, B. I. Halperin, and I. M. Ruzin, *Phys. Rev. B* **55**, 2344 (1997).
 - [29] M. Sigrist and K. Ueda, *Rev. Mod. Phys.* **63**, 239 (1991).
 - [30] A. Larkin and A. Varlamov, *Theory of Fluctuations in Superconductors* (Oxford University Press, 2009).
 - [31] Supplemental Material.
 - [32] M. Khodas and A. M. Finkel'stein, *Phys. Rev. B* **68**, 155114 (2003).
 - [33] K. Michaeli, K. S. Tikhonov, and A. M. Finkel'stein, *Phys. Rev. B* **86**, 014515 (2012).
 - [34] E. Helfand and N. R. Werthamer, *Phys. Rev.* **147**, 288 (1966).
 - [35] F. Bourdarot, B. Fåk, K. Habicht, and K. Prokeš, *Phys. Rev. Lett.* **90**, 067203 (2003).
 - [36] C. R. Wiebe, J. A. Janik, G. J. MacDougall, G. M. Luke, J. D. Garrett, H. D. Zhou, Y.-J. Jo, L. Balicas, Y. Qiu, J. R. D. Copley, et al., *Nature Phys.* **3**, 96 (2007).
 - [37] V. M. Galitski and A. I. Larkin, *Phys. Rev. B* **63**, 174506 (2001).
 - [38] I. Ussishkin, *Phys. Rev. B* **68**, 024517 (2003).
 - [39] M. Serbyn, M. Skvortsov, A. Varlamov, and V. Galitski, *Phys. Rev. Lett.* **102**, 067001 (2009).
 - [40] K. Michaeli and A. M. Finkel'stein, *EPL (Europhysics Letters)* **86**, 27007 (2009).
 - [41] We used the parameters of the material: $T_c \sim 1.5\text{K}$, $k_F \sim 0.5 \cdot 10^{10}\text{m}^{-1}$, $v_F \sim 1 \cdot 10^4\text{m/s}$ [46], and $\Gamma \sim 1.5\text{meV}$ [35, 36], and set the cutoff momentum as $\Lambda = 1/\xi$. We neglected the τ -dependence of the transition temperature T_c and coherence length ξ . These assumptions are justified for $T\tau \gg 1$. In this letter, RRR is defined as the ratio of $\sigma_{xx}(T = 300\text{K})$ to $\sigma_{xx}(T = 0\text{K})$, which is obtain by extrapolating the temperature dependence of the conductivity in the normal-metal region to $T = 0$ K. It is also assumed that the longitudinal conductivity obeys $\sigma_{xx} \propto \tau^{-1} = \tau_{imp}^{-1} + AT^2$, where τ_{imp} and A are T -independent constant.
 - [42] A. G. Aronov, S. Hikami, and A. I. Larkin, *Phys. Rev. B* **51**, 3880 (1995).
 - [43] Sinitsyn, N. A. and MacDonald, A. H. and Jungwirth, T. and Dugaev, V. K. and Sinova, Jairo, *Phys. Rev. B* **75**, 045315 (2007).
 - [44] T. Yamashita, S. Tonegawa, Y. Tsuruhara, Y. Shimoyama, T. Shibauchi, and Y. Matsuda (Private Communication); They measured the ab -plane Nernst coefficient

cients of highly clean URu₂Si₂ samples with RRR ~ 600 and 1000 under magnetic fields parallel to the c -axis. Their data show quite anomalous behaviors which can not be explained by standard theories, but, remarkably, coincide with our theoretical predictions.

- [45] F. Rullier-Albenque, R. Tourbot, H. Alloul, P. Lejay, D. Colson, and A. Forget, Phys. Rev. Lett. **96**, 067002 (2006).
 [46] W. Schlitz, J. Baumann, B. Pollit, U. Rauchschwalbe, H. Mayer, U. Ahlheim, and C. Bredl, Z. Phys. B **62**, 171 (1986).

Supplemental Material

A. BPS under Magnetic Field

In this section, we derive the expression of the BPS (3) under a homogeneous magnetic field $(0, 0, H)$.

The interaction term of the Hamiltonian (2) for the chirality $C = +1$ channel can be rewritten in real-space representation as:

$$\begin{aligned} H^{int} &= -g \int d\mathbf{r} \left[V^+ \left(\frac{-i(\partial_1 - \partial_2)}{2}, \frac{-i(\partial'_1 - \partial'_2)}{2} \right) \right. \\ &\quad \left. c_{\uparrow}^*(\mathbf{r}_1) c_{\downarrow}^*(\mathbf{r}_2) c_{\downarrow}(\mathbf{r}'_2) c_{\uparrow}(\mathbf{r}'_1) \right]_{\mathbf{r}_1, \mathbf{r}_2, \mathbf{r}'_1, \mathbf{r}'_2 \rightarrow \mathbf{r}} \\ &= -g \int d\mathbf{r} \left[\phi \left(\frac{-i(\partial_1 - \partial_2)}{2} \right) \phi^\dagger \left(\frac{-i(\partial'_1 - \partial'_2)}{2} \right) \right. \\ &\quad \left. c_{\uparrow}^*(\mathbf{r}_1) c_{\downarrow}^*(\mathbf{r}_2) c_{\downarrow}(\mathbf{r}'_2) c_{\uparrow}(\mathbf{r}'_1) \right]_{\mathbf{r}_1, \mathbf{r}_2, \mathbf{r}'_1, \mathbf{r}'_2 \rightarrow \mathbf{r}}. \end{aligned} \quad (\text{S.9})$$

Therefore, the BPS of this channel is given by,

$$\begin{aligned} \tilde{\Pi}_{C=1}(\mathbf{x}, \mathbf{y}, \omega_l; H) &= T \sum_{\varepsilon_n} \left[\phi \left(\frac{-i(\partial_1 - \partial_2)}{2} \right) \phi^\dagger \left(\frac{-i(\partial'_1 - \partial'_2)}{2} \right) \right. \\ &\quad \left. \tilde{G}(\mathbf{r}'_1, \mathbf{r}_1, \varepsilon_{n+l}; H) \tilde{G}(\mathbf{r}'_2, \mathbf{r}_2, -\varepsilon_n; H) \right] \Big|_{\substack{\mathbf{r}'_1, \mathbf{r}'_2 \rightarrow \mathbf{x}, \\ \mathbf{r}_1, \mathbf{r}_2 \rightarrow \mathbf{y}}}. \end{aligned} \quad (\text{S.10})$$

In the presence of a uniform magnetic field, the one-particle Green function is $\tilde{G}(\mathbf{r}', \mathbf{r}, \varepsilon_n; H) = e^{-ie\Phi(\mathbf{r}', \mathbf{r})} G_{core}(\mathbf{r}' - \mathbf{r}, \varepsilon_n; H)$, where $\Phi(\mathbf{x}, \mathbf{y}) = \int_{\mathbf{x}}^{\mathbf{y}} \mathbf{A}(\mathbf{r}) d\mathbf{r}$ is an integral of the vector potential $\mathbf{A}(\mathbf{r})$ along a straight line, and $G_{core}(\mathbf{r}' - \mathbf{r}, \varepsilon_n; H)$ is the “core” Green function, which is translation (then it is a function of $\mathbf{r}' - \mathbf{r}$), c -axis rotation, and gauge invariant [32, 33], and is given as the solution of

$$\left[i\varepsilon_n - \frac{1}{2m} (-i\nabla_{\rho} + \frac{e}{2} \boldsymbol{\rho} \times \mathbf{H})^2 + \mu - \hat{\Sigma} \right] G_{core}(\boldsymbol{\rho}, \varepsilon_n; H) = \delta(\boldsymbol{\rho}), \quad (\text{S.11})$$

where $\boldsymbol{\rho} = \mathbf{r}' - \mathbf{r}$, and $\hat{\Sigma}$ is the self-energy that also has the same symmetries as mentioned above.

To proceed further, we take the Landau gauge, $\mathbf{A}(\mathbf{r}) = (0, xH, 0)$, although the final results (S.12), (S.13), and (S.14) are correct for any gauge choice as shown in the last part of this section. For this gauge, $\Phi(\mathbf{r}', \mathbf{r}) = \frac{eH}{2}(x' + x)(y - y')$. Now, we introduce the pairing symmetry function of p_z -wave superconductors, $\phi^z(\mathbf{k}) = \sqrt{3}k_z/k_F$, and let $\theta = -ie(\Phi(\mathbf{r}'_1, \mathbf{r}_1) + \Phi(\mathbf{r}'_2, \mathbf{r}_2))$, $\phi_{12} = \phi \left(\frac{-i(\partial_1 - \partial_2)}{2} \right)$, and $\phi_{12}^z = \phi^z \left(\frac{-i(\partial_1 - \partial_2)}{2} \right)$. The commutations of ϕ and θ are given by $[\phi_{12}, \theta] = \frac{1}{4} \sqrt{\frac{5}{2}} \frac{ieH}{k_F} (-x_1 - x'_1 + x_2 + x'_2 + iy_1 - iy'_1 - iy'_2 + iy'_2) \phi_{12}^z$, $[\phi_{12}^\dagger, \theta] = \frac{1}{4} \sqrt{\frac{5}{2}} \frac{ieH}{k_F} (-x_1 - x'_1 + x_2 + x'_2 + iy_1 - iy'_1 - iy'_2 + iy'_2) \phi_{12}^z$, and $[\phi_{12}, [\phi_{12}^\dagger, \theta]] = -\frac{5eH}{4k_F^2} \phi_{12}^z \phi_{12}^z$. Then, $[\phi_{12}, \theta] \rightarrow 0$ and $[\phi_{12}^\dagger, \theta] \rightarrow 0$ as $\mathbf{r}'_1, \mathbf{r}'_2 \rightarrow \mathbf{x}$ and $\mathbf{r}_1, \mathbf{r}_2 \rightarrow \mathbf{y}$. By using these commutation relations and the formulae $e^B A e^{-B} = A + [B, A] + [B, [B, A]] + \dots$ and $[PQ, R] = P[Q, R] + [P, R]Q$, we obtain

$$\begin{aligned} \tilde{\Pi}_{C=1}(\mathbf{x}, \mathbf{y}, \omega_q; H) &= e^{-2ie\Phi(\mathbf{x}, \mathbf{y})} \\ &\quad \left[T \sum_{\varepsilon_n} \phi_{12} \phi_{12}^\dagger G_{core}(\mathbf{r}'_1 - \mathbf{r}_1, \varepsilon_{n+q}; H) G_{core}(\mathbf{r}'_2 - \mathbf{r}_2, -\varepsilon_n; H) \right. \\ &\quad \left. - \frac{5eH}{4k_F^2} T \sum_{\varepsilon_n} \phi_{12}^z \phi_{12}^z G_{core}(\mathbf{r}'_1 - \mathbf{r}_1, \varepsilon_{n+q}; H) \right. \\ &\quad \left. G_{core}(\mathbf{r}'_2 - \mathbf{r}_2, -\varepsilon_n; H) \right]_{\substack{\mathbf{r}'_1, \mathbf{r}'_2 \rightarrow \mathbf{x}, \\ \mathbf{r}_1, \mathbf{r}_2 \rightarrow \mathbf{y}}} \\ &= e^{-i2e\Phi(\mathbf{x}, \mathbf{y})} \\ &\quad \left[\Pi(\mathbf{x} - \mathbf{y}, \omega_q; H) - \frac{5eH}{4k_F^2} \Pi'(\mathbf{x} - \mathbf{y}, \omega_q; H) \right], \end{aligned} \quad (\text{S.12})$$

where

$$\begin{aligned} \Pi(\boldsymbol{\rho}, \omega_q; H) &= \left[T \sum_{\varepsilon_n} |\phi|^2 \left(\frac{-i(\partial_{\rho_1} - \partial_{\rho_2})}{2} \right) G_{core}(\boldsymbol{\rho}_1, \varepsilon_{n+q}; H) \right. \\ &\quad \left. G_{core}(\boldsymbol{\rho}_2, -\varepsilon_n; H) \right]_{\boldsymbol{\rho}_1, \boldsymbol{\rho}_2 \rightarrow \boldsymbol{\rho}}, \end{aligned} \quad (\text{S.13})$$

$$\begin{aligned} \Pi'(\boldsymbol{\rho}, \omega_q; H) &= \left[T \sum_{\varepsilon_n} |\phi^z|^2 \left(\frac{-i(\partial_{\rho_1} - \partial_{\rho_2})}{2} \right) G_{core}(\boldsymbol{\rho}_1, \varepsilon_{n+q}; H) \right. \\ &\quad \left. G_{core}(\boldsymbol{\rho}_2, -\varepsilon_n; H) \right]_{\boldsymbol{\rho}_1, \boldsymbol{\rho}_2 \rightarrow \boldsymbol{\rho}} \end{aligned} \quad (\text{S.14})$$

are “core” BPSs, which preserve spatial translation, c -axis rotation, and gauge invariances. Here $|\phi(\mathbf{k})|^2 = 15k_z^2(k_x^2 + k_y^2)/2k_F^4$ and $|\phi^z(\mathbf{k})|^2 = 3k_z^2/k_F^2$. Then, we arrive at Eq.(3) for $C = +1$. Carrying out similar calculations with the effective interaction term V^- , we can obtain Eq.(3) for $C = -1$.

So far we have used the Landau gauge. However, by using the formulae, $[\phi_{12}, e^{-i(\chi(\mathbf{r}_1) + \chi(\mathbf{r}_2))}]_{\substack{\mathbf{r}'_1, \mathbf{r}'_2 \rightarrow \mathbf{x} \\ \mathbf{r}_1, \mathbf{r}_2 \rightarrow \mathbf{y}}} = 0$, and so on, with χ an arbitrary function, we can prove that

the final results, (S.12), (S.13), and (S.14), are gauge invariant.

B. Nernst and Hall Conductivities

In this section, we present the derivation of the Nernst and Hall conductivities for the ANE and AHE caused by the Berry-phase fluctuation mechanism, (4) and (5).

Formally, to obtain the whole contributions from the superconducting fluctuations to the Kubo term of the Peltier coefficient and the Hall coefficient, one has to evaluate all possible Feynman diagrams that consist of two current vertices, superconducting fluctuation propagators, \tilde{L}_C , and Green functions, \tilde{G} , in a magnetic field. We focus on the case with a weak magnetic field, where the Nernst and Hall conductivities are linear in H . Up to the linear order of H , the fluctuation propagator (3) is divided into two term:

$$\tilde{L}_C = \tilde{L}_0 + \tilde{L}'_C + \mathcal{O}(H^2), \quad (\text{S.15})$$

where

$$\begin{aligned} & \tilde{L}_0^{-1}(\mathbf{x}, \mathbf{y}, \omega_q; H) \\ &= -\frac{\delta(\mathbf{x} - \mathbf{y})}{g} + e^{-i2e\Phi(\mathbf{x}, \mathbf{y})} \Pi(\mathbf{x} - \mathbf{y}, \omega_q; H) \end{aligned} \quad (\text{S.16})$$

is the conventional part of the fluctuation propagator, and

$$\tilde{L}'_C(\mathbf{x} - \mathbf{y}, \omega_q; H) = C \cdot \left(\frac{5eH}{4k_F^2 g} \right) [L(\mathbf{x} - \mathbf{y}, \omega_q)]^2 \quad (\text{S.17})$$

is the chirality-dependent one which is characteristic of chiral superconductors. Here $L(\mathbf{x} - \mathbf{y}, \omega_q)$ is the fluctuation propagator of $d_{zx} \pm id_{zy}$ -wave channel in zero magnetic field. The concrete expression of $L(\mathbf{x} - \mathbf{y}, \omega_q)$ and its derivation are given in Sec.C. From Eq.(S.15), we see that in the linear order of H , the whole contributions to the Nernst and Hall conductivities are separated into two parts: [A] contribution from diagrams which do not include the chirality-dependent fluctuation propagator, \tilde{L}'_C , [B] contribution from diagrams which include one chirality-dependent fluctuation propagator \tilde{L}'_C .

The contribution [A] also appears for the case of non-chiral superconductors, such as s - and $d_{x^2-y^2}$ -wave pairings, which can be described by conventional theories [30, 38, 39], and, therefore, physically, this part corresponds to the contributions due to Lorentz force on quasi-particles and fluctuating Cooper pairs. On the other hand, [B] is unique to chiral superconductors, raised by chirality-polarization, and as shown below, associated with the ANE and AHE caused by the Berry-phase fluctuation mechanism without Lorentz force.

From now on, we concentrate on the latter contribution, and write down the correlation functions for the

Nernst and Hall conductivities in the form,

$$A_{xy}(\omega_l) = -2eT \sum_{\mathbf{q}, \omega_q, C=\pm 1} \tilde{L}'_C(\mathbf{q}, \omega_q; H) \bar{A}_C(\mathbf{q}, \omega_q; \omega_l), \quad (\text{S.18})$$

where only the odd part of \bar{A}_C with respect to time reversal: $C \rightarrow -C$, gives nonzero contributions, since \tilde{L}'_C is odd.

We examine the leading-order diagrams belonging to [B], which give the dominant contribution. It is found that the three diagrams which give leading-order contributions in conventional theories, i.e. the Aslamazov-Larkin (AL), Maki-Thompson (MT), and density-of-states (DOS) diagrams (upper panel in FIG. 1) do not contribute in this case, and generally, all contributions from diagrams belonging to the classes of the lower panel in FIG. 1 are zero. The reason is that in these diagrams the pairing function appear as $|\phi|^2$, and, therefore, their contributions to \bar{A}_C have only even part with respect to time reversal:

$$\bar{A}_C^{AL, MT, DOS} = \bar{A}_{-C}^{AL, MT, DOS}, \quad (\text{S.19})$$

which do not contribute to the correlation function as mentioned above. The lowest order diagrams which do not belong to these classes and give nonzero contributions are depicted in FIG. 2 in the main text. For clarity, we depicted them more explicitly in FIGs. S.4a-c). In these diagrams, a renormalized four-point vertex, $W(\mathbf{k}, \omega_k)$, (double line) raised by electron-electron interaction is inserted. To proceed further, we introduce a simple model: $W(\mathbf{k}, \omega_k) = W_0/(1 + |\omega_k|/\Gamma)$, the four-point vertex mediated via the short-range spin fluctuation, where we discuss about the assumption in Sec. F.

Now, we calculate contributions from diagrams $a)$, $b)$, $c)$, and their mirror images in FIG. 2 to the Kubo terms of the Nernst conductivity, $\alpha_{xy}^{(i) Kubo}$, ($i = a, b$, and c), and the Hall conductivity, $\sigma_{xy}^{(i)}$, ($i = a, b$, and c). They are, respectively, given by

$$\alpha_{xy}^{(i) Kubo} = \frac{1}{T} \frac{A_{\alpha\beta}^{(i) R}(\omega)}{(-i\omega)} \bigg|_{\omega \rightarrow 0}, \quad (\text{S.20})$$

$$\sigma_{xy}^{(i)} = \frac{S_{\alpha\beta}^{(i) R}(\omega)}{(-i\omega)} \bigg|_{\omega \rightarrow 0}, \quad (\text{S.21})$$

where $A_{\alpha\beta}^{(i) R}(\omega)$ is the retarded correlation function of heat currents, and $S_{\alpha\beta}^{(i) R}(\omega)$ is that of charge currents. Their corresponding correlation functions with the Matsubara frequencies are, respectively,

$$A_{xy}^i(\omega_l) = -2eT \sum_{\omega_q, \mathbf{q}, C=\pm 1} \tilde{L}'_C(\mathbf{q}, \omega_q; H) \bar{A}_C^i(\mathbf{q}, \omega_q; \omega_l), \quad (\text{S.22})$$

$$S_{xy}^i(\omega_l) = 2e^2T \sum_{\omega_q, \mathbf{q}, C=\pm 1} \tilde{L}'_C(\mathbf{q}, \omega_q; H) \bar{S}_C^i(\mathbf{q}, \omega_q; \omega_l), \quad (\text{S.23})$$

where ω_q and ω_l are the Matsubara frequencies, and \mathbf{q} is a wave number. Here,

$$\begin{aligned} \bar{A}_{C=1}^i(\mathbf{q}, \omega_q; \omega_l) \\ = -2T^2 \text{Re} \left[\sum_{n,m} X^i(\mathbf{q}, n, \omega_q; \omega_l) Y^i(\mathbf{q}, m, \omega_q; \omega_l) \right. \\ \left. \frac{W_0}{1 + |\omega_{n-m}|/\Gamma} \right], \end{aligned} \quad (\text{S.24})$$

$$\begin{aligned} \bar{S}_{C=1}^i(\mathbf{q}, \omega_q; \omega_l) \\ = -2T^2 \text{Re} \left[\sum_{n,m} X^i(\mathbf{q}, n, \omega_q; \omega_l) Z^i(\mathbf{q}, m, \omega_q; \omega_l) \right. \\ \left. \frac{W_0}{1 + |\omega_{n-m}|/\Gamma} \right], \end{aligned} \quad (\text{S.25})$$

and

$$\begin{aligned} X^a(\mathbf{q}, n, \omega_q; \omega_l) \\ = \sum_{\mathbf{p}} \phi^\dagger(\mathbf{p} - \frac{\mathbf{q}}{2}) G(\mathbf{q} - \mathbf{p}, -\varepsilon_{n-l-q}) G(\mathbf{p}, \varepsilon_{n-l}) \\ G(\mathbf{p}, \varepsilon_n) v_x(\mathbf{p}), \end{aligned} \quad (\text{S.26})$$

$$\begin{aligned} Y^a(\mathbf{q}, m, \omega_q; \omega_l) \\ = \sum_{\mathbf{s}} \phi(\mathbf{s} - \frac{\mathbf{q}}{2}) G(\mathbf{q} - \mathbf{s}, -\varepsilon_{m-l-q}) G(\mathbf{s}, \varepsilon_{m-l}) \\ G(\mathbf{s}, \varepsilon_m) \frac{i(\varepsilon_{m-l} + \varepsilon_m)}{2} v_y(\mathbf{s}), \end{aligned} \quad (\text{S.27})$$

$$\begin{aligned} Z^a(\mathbf{q}, m, \omega_q; \omega_l) \\ = \sum_{\mathbf{s}} \phi(\mathbf{s} - \frac{\mathbf{q}}{2}) G(\mathbf{q} - \mathbf{s}, -\varepsilon_{m-l-q}) G(\mathbf{s}, \varepsilon_{m-l}) \\ G(\mathbf{s}, \varepsilon_m) v_y(\mathbf{s}), \end{aligned} \quad (\text{S.28})$$

$$\begin{aligned} X^b(\mathbf{q}, n, \omega_q; \omega_l) \\ = \sum_{\mathbf{p}} \phi^\dagger(\mathbf{p} + \frac{\mathbf{q}}{2}) G(\mathbf{q} + \mathbf{p}, \varepsilon_n) G(-\mathbf{p}, -\varepsilon_{n-q}) \\ G(-\mathbf{p}, -\varepsilon_{n-q-l}) v_x(-\mathbf{p}), \end{aligned} \quad (\text{S.29})$$

$$\begin{aligned} Y^b(\mathbf{q}, m, \omega_q; \omega_l) \\ = \sum_{\mathbf{s}} \phi(\mathbf{s} - \frac{\mathbf{q}}{2}) G(\mathbf{q} - \mathbf{s}, -\varepsilon_{m-q-l}) G(\mathbf{s}, \varepsilon_{m-l}) \\ G(\mathbf{s}, \varepsilon_m) \frac{i(\varepsilon_m + \varepsilon_{m-l})}{2} v_y(\mathbf{s}), \end{aligned} \quad (\text{S.30})$$

$$\begin{aligned} Z^b(\mathbf{q}, m, \omega_q; \omega_l) \\ = \sum_{\mathbf{s}} \phi(\mathbf{s} - \frac{\mathbf{q}}{2}) G(\mathbf{q} - \mathbf{s}, -\varepsilon_{m-q-l}) G(\mathbf{s}, \varepsilon_{m-l}) \\ G(\mathbf{s}, \varepsilon_m) v_y(\mathbf{s}), \end{aligned} \quad (\text{S.31})$$

$$\begin{aligned} X^c(\mathbf{q}, n, \omega_q; \omega_l) \\ = \sum_{\mathbf{p}} \phi^\dagger(\mathbf{p} - \frac{\mathbf{q}}{2}) G(\mathbf{q} - \mathbf{p}, -\varepsilon_{n+l-q}) G(\mathbf{p}, \varepsilon_{n+l}), \end{aligned} \quad (\text{S.32})$$

$$\begin{aligned} Y^c(\mathbf{q}, m, \omega_q; \omega_l) \\ = \sum_{\mathbf{s}} \phi(\mathbf{s} - \frac{\mathbf{q}}{2}) G(\mathbf{q} - \mathbf{s}, -\varepsilon_{m-q}) G(\mathbf{s}, \varepsilon_m) G(\mathbf{s}, \varepsilon_{m+l}) \\ G(\mathbf{q} - \mathbf{s}, -\varepsilon_{m+l-q}) v_x(\mathbf{q} - \mathbf{s}) \frac{i(\varepsilon_m + \varepsilon_{m+l})}{2} v_y(\mathbf{s}), \end{aligned} \quad (\text{S.33})$$

$$\begin{aligned} Z^c(\mathbf{q}, m, \omega_q; \omega_l) \\ = \sum_{\mathbf{s}} \phi(\mathbf{s} - \frac{\mathbf{q}}{2}) G(\mathbf{q} - \mathbf{s}, -\varepsilon_{m-q}) G(\mathbf{s}, \varepsilon_m) G(\mathbf{s}, \varepsilon_{m+l}) \\ G(\mathbf{q} - \mathbf{s}, -\varepsilon_{m+l-q}) v_x(\mathbf{q} - \mathbf{s}) v_y(\mathbf{s}). \end{aligned} \quad (\text{S.34})$$

We can also obtain the expressions for $\bar{A}_{C=-1}^i$ and $\bar{S}_{C=-1}^i$ by using chirality-inversion (time-reversal) transformation, $\phi \rightarrow \phi^\dagger$ and $\phi^\dagger \rightarrow \phi$ in X^i , Y^i , and Z^i , of Eqs. (S.24-S.34). In the above equations, the one-particle Green function, chiral $d_{zx} + id_{zy}$ -wave pairing symmetry function, and velocity of quasiparticles are defined as $G(\mathbf{k}, \varepsilon_k)^{-1} = i\tilde{\varepsilon}_k - \xi_{\mathbf{k}} = i(\varepsilon_k + \text{sgn}(\varepsilon_k)/2\tau) - \xi_{\mathbf{k}}$, $\phi(\mathbf{k}) = \sqrt{15/2} k_z (k_x + ik_y)/k_F^2$, and $\mathbf{v}(\mathbf{k}) = \partial \xi_{\mathbf{k}} / \partial \mathbf{k}$, respectively. Here τ is the relaxation time of quasiparticles. For simplicity, we take the spherical Fermi surface: $\xi_{\mathbf{k}} = k^2/2m - \mu$, where m and μ are the mass and chemical potential of the quasiparticles, respectively.

We, henceforth, neglect quantum superconducting fluctuations keeping only terms with $\omega_q = 0$. Since singular contributions at T_c come from long-wave length regions where the center-of-mass momentum of fluctuating Cooper pairs q is small, we concentrate on the analysis of \bar{A}^i and \bar{S}^i for small q . Then, expanding X^i , Y^i , and Z^i as power series of q/k_F , we obtain

$$\begin{aligned} X^a(\mathbf{q}, n, \omega_q = 0; \omega_l) \\ = N(0) q_z \left[i\pi \sqrt{\frac{5}{24}} \frac{v_F}{k_F} \frac{\text{sgn}(n+1/2)}{(|\tilde{\varepsilon}_n| + |\tilde{\varepsilon}_{n-l}|)|\tilde{\varepsilon}_{n-l}|} \right. \\ \left. - \frac{\pi}{2} \sqrt{\frac{1}{30}} v_F^2 \left\{ \frac{|\tilde{\varepsilon}_n| + 3|\tilde{\varepsilon}_{n-l}|}{|\tilde{\varepsilon}_{n-l}|^2 (|\tilde{\varepsilon}_n| + |\tilde{\varepsilon}_{n-l}|)^2}, \right. \right. \\ \left. \left. \begin{array}{l} \text{for } (n-l+1/2)(n+1/2) > 0 \\ -1 \\ \text{for } (n-l+1/2)(n+1/2) < 0 \end{array} \right\} \right] \\ + \mathcal{O} \left(\left(\frac{q}{k_F} \right)^2 \right), \end{aligned} \quad (\text{S.35})$$

$$\begin{aligned} Y^a(\mathbf{q}, m, \omega_q = 0; \omega_l) \\ = -\frac{(\varepsilon_{m-l} + \varepsilon_m)}{2} X^a(\mathbf{q}, m, \omega_q = 0; \omega_l), \end{aligned} \quad (\text{S.36})$$

$$\begin{aligned} Z^a(\mathbf{q}, m, \omega_q = 0; \omega_l) \\ = iX^a(\mathbf{q}, m, \omega_q = 0; \omega_l), \end{aligned} \quad (\text{S.37})$$

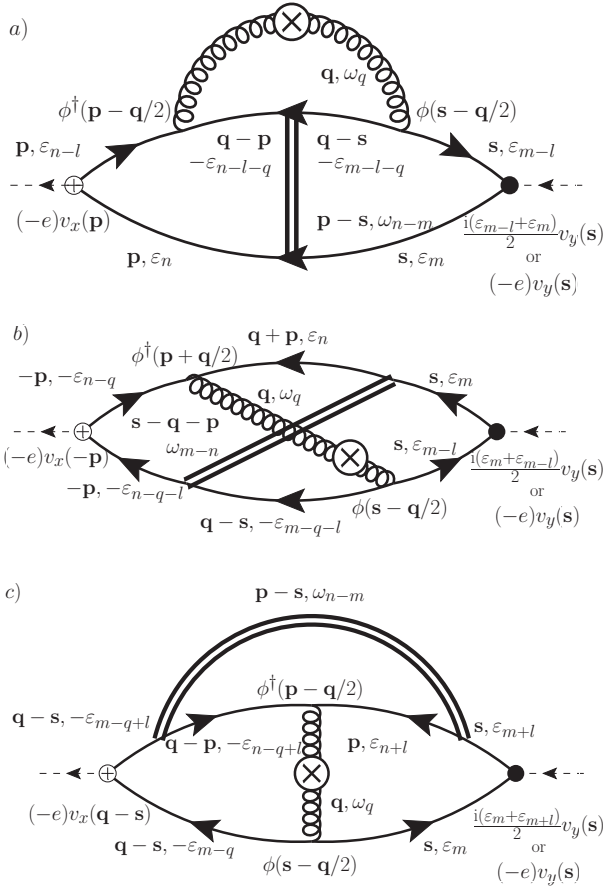


FIG. S.4: Diagrams a), b), and c) of FIG. 2 with wave numbers and frequencies explicitly shown.

$$\begin{aligned}
X^b(\mathbf{q}, n, \omega_q = 0; \omega_l) &= N(0)q_z \left[-i\pi \sqrt{\frac{5}{24}} \frac{v_F}{k_F} \frac{\text{sgn}(n-l+1/2)}{(|\tilde{\varepsilon}_n| + |\tilde{\varepsilon}_{n-l}|)|\tilde{\varepsilon}_n|} \right. \\
&\quad \left. - \frac{\pi}{2} \sqrt{\frac{1}{30}} v_F^2 \left\{ \frac{|\tilde{\varepsilon}_{n-l}| + 3|\tilde{\varepsilon}_n|}{|\tilde{\varepsilon}_n|^2(|\tilde{\varepsilon}_{n-l}| + |\tilde{\varepsilon}_n|)^2}, \text{ for } (n-l+1/2)(n+1/2) > 0 \right. \right. \\
&\quad \left. \left. -1 \right. \right. \\
&\quad \left. \left. \frac{|\tilde{\varepsilon}_n|^2(|\tilde{\varepsilon}_{n-l}| + |\tilde{\varepsilon}_n|)}{|\tilde{\varepsilon}_{n-l}|^2(|\tilde{\varepsilon}_n| + |\tilde{\varepsilon}_{n-l}|)}, \text{ for } (n-l+1/2)(n+1/2) < 0 \right\} \right] \\
&\quad + \mathcal{O}\left(\left(\frac{q}{k_F}\right)^2\right), \tag{S.38}
\end{aligned}$$

$$\begin{aligned}
Y^b(\mathbf{q}, m, \omega_q = 0; \omega_l) &= N(0)q_z \frac{\varepsilon_m + \varepsilon_{m-l}}{2} \left[-i\pi \sqrt{\frac{5}{24}} \frac{v_F}{k_F} \frac{\text{sgn}(m+1/2)}{(|\tilde{\varepsilon}_m| + |\tilde{\varepsilon}_{m-l}|)|\tilde{\varepsilon}_{m-l}|} \right. \\
&\quad \left. + \frac{\pi}{2} \sqrt{\frac{1}{30}} v_F^2 \left\{ \frac{|\tilde{\varepsilon}_m| + 3|\tilde{\varepsilon}_{m-l}|}{|\tilde{\varepsilon}_{m-l}|^2(|\tilde{\varepsilon}_m| + |\tilde{\varepsilon}_{m-l}|)^2}, \text{ for } (m-l+1/2)(m+1/2) > 0 \right. \right. \\
&\quad \left. \left. -1 \right. \right. \\
&\quad \left. \left. \frac{|\tilde{\varepsilon}_{m-l}|^2(|\tilde{\varepsilon}_m| + |\tilde{\varepsilon}_{m-l}|)}{|\tilde{\varepsilon}_m|^2(|\tilde{\varepsilon}_{m-l}| + |\tilde{\varepsilon}_m|)}, \text{ for } (m-l+1/2)(m+1/2) < 0 \right\} \right] \\
&\quad + \mathcal{O}\left(\left(\frac{q}{k_F}\right)^2\right), \tag{S.39}
\end{aligned}$$

$$\begin{aligned}
Z^b(\mathbf{q}, m, \omega_q = 0; \omega_l) &= N(0)q_z \left[-\pi \sqrt{\frac{5}{24}} \frac{v_F}{k_F} \frac{\text{sgn}(m+1/2)}{(|\tilde{\varepsilon}_m| + |\tilde{\varepsilon}_{m-l}|)|\tilde{\varepsilon}_{m-l}|} \right. \\
&\quad \left. - i\frac{\pi}{2} \sqrt{\frac{1}{30}} v_F^2 \left\{ \frac{|\tilde{\varepsilon}_m| + 3|\tilde{\varepsilon}_{m-l}|}{|\tilde{\varepsilon}_{m-l}|^2(|\tilde{\varepsilon}_m| + |\tilde{\varepsilon}_{m-l}|)^2}, \text{ for } (m-l+1/2)(m+1/2) > 0 \right. \right. \\
&\quad \left. \left. -1 \right. \right. \\
&\quad \left. \left. \frac{|\tilde{\varepsilon}_{m-l}|^2(|\tilde{\varepsilon}_m| + |\tilde{\varepsilon}_{m-l}|)}{|\tilde{\varepsilon}_m|^2(|\tilde{\varepsilon}_{m-l}| + |\tilde{\varepsilon}_m|)}, \text{ for } (m-l+1/2)(m+1/2) < 0 \right\} \right] \\
&\quad + \mathcal{O}\left(\left(\frac{q}{k_F}\right)^2\right), \tag{S.40}
\end{aligned}$$

$$X^c(\mathbf{q}, n, \omega_q = 0; \omega_l) = \mathcal{O}\left(\left(\frac{q}{k_F}\right)^2\right), \tag{S.41}$$

$$Y^c(\mathbf{q}, m, \omega_q = 0; \omega_l) = \mathcal{O}\left(\frac{q}{k_F}\right), \tag{S.42}$$

$$Z^c(\mathbf{q}, m, \omega_q = 0; \omega_l) = \mathcal{O}\left(\frac{q}{k_F}\right), \tag{S.43}$$

for $\omega_l > 0$, where $N(0)$ is the density-of-states at the Fermi surface. Since $\bar{A}_{C=1}^c(\mathbf{q}, \omega_q = 0; \omega_l) = \mathcal{O}\left(\left(\frac{q}{k_F}\right)^3\right)$, and $\bar{S}_{C=1}^c(\mathbf{q}, \omega_q = 0; \omega_l) = \mathcal{O}\left(\left(\frac{q}{k_F}\right)^3\right)$, the contribution from the c) diagram is less singular near T_c than that from a) or b). Therefore, we neglect the contributions from this diagram.

The most singular part in DC limit for a clean system with large τ arises from the summation over n in the region $n, m = 0, 1, \dots, l-1$, where $|\tilde{\varepsilon}_n| + |\tilde{\varepsilon}_{n-l}| = \omega_l + 1/\tau$. We take only such terms and obtain

$$\begin{aligned}
\bar{A}_{C=1}^a(\mathbf{q}, \omega_q = 0; \omega_l) &= \frac{N(0)^2 W_0 q_z^2}{(\omega_l + 1/\tau)^2} \sum_{0 \leq n, m \leq l-1} \frac{1}{1 + (2\pi T/\Gamma)|n-m|} \\
&\quad \times \left\{ -\frac{5\pi}{48} \frac{T v_F^2}{k_F^2} \frac{2m-l+1}{(n-l+1/2-1/4\pi\tau T)(m-l+1/2-1/4\pi\tau T)} \right. \\
&\quad \left. + \frac{1}{960\pi} \frac{v_F^4}{T} \frac{2m-l+1}{(n-l+1/2-1/4\pi\tau T)^2(m-l+1/2-1/4\pi\tau T)^2} \right\}, \tag{S.44}
\end{aligned}$$

$$\begin{aligned}
& \bar{A}_{C=1}^b(\mathbf{q}, \omega_q = 0; \omega_l) \\
&= \frac{N(0)^2 W_0 q_z^2}{(\omega_l + 1/\tau)^2} \sum_{0 \leq n, m \leq l-1} \frac{1}{1 + (2\pi T/\Gamma)|n-m|} \\
&\times \left\{ -\frac{5\pi}{48} \frac{T v_F^2}{k_F^2} \frac{2m-l+1}{(n+1/2+1/4\pi\tau T)(m-l+1/2-1/4\pi\tau T)} \right. \\
&\left. + \frac{1}{960\pi} \frac{v_F^4}{T} \frac{2m-l+1}{(n+1/2+1/4\pi\tau T)^2(m-l+1/2-1/4\pi\tau T)^2} \right\}, \quad (\text{S.45})
\end{aligned}$$

$$\begin{aligned}
& \bar{S}_{C=1}^a(\mathbf{q}, \omega_q = 0; \omega_l) \\
&= \frac{N(0)^2 W_0 q_z^2}{(\omega_l + 1/\tau)^2} \sum_{0 \leq n, m \leq l-1} \frac{1}{1 + (2\pi T/\Gamma)|n-m|} \\
&\times \frac{-1}{48\pi} \frac{v_F^3}{k_F T} \frac{1}{(n-l+1/2-1/4\pi\tau T)(m-l+1/2-1/4\pi\tau T)^2}, \quad (\text{S.46})
\end{aligned}$$

$$\begin{aligned}
& \bar{S}_{C=1}^b(\mathbf{q}, \omega_q = 0; \omega_l) \\
&= \frac{N(0)^2 W_0 q_z^2}{(\omega_l + 1/\tau)^2} \sum_{0 \leq n, m \leq l-1} \frac{1}{1 + (2\pi T/\Gamma)|n-m|} \\
&\times \frac{1}{48\pi} \frac{v_F^3}{k_F T} \frac{1}{(n+1/2+1/4\pi\tau T)(m-l+1/2-1/4\pi\tau T)^2}. \quad (\text{S.47})
\end{aligned}$$

Up to now, we have calculated only the $C = 1$ terms. However, by carrying out calculations similar to (S.26-S.47), we immediately find,

$$\bar{A}_{C=-1}^i(\mathbf{q}, \omega_q = 0; \omega_l) = -\bar{A}_{C=1}^i(\mathbf{q}, \omega_q = 0; \omega_l), \quad (\text{S.48})$$

$$\bar{S}_{C=-1}^i(\mathbf{q}, \omega_q = 0; \omega_l) = -\bar{S}_{C=1}^i(\mathbf{q}, \omega_q = 0; \omega_l). \quad (\text{S.49})$$

Now, we introduce $\bar{\alpha}_C^i(\mathbf{q}), \bar{\sigma}_C^i(\mathbf{q})$ ($i = a, b$, and c) defined as,

$$\begin{aligned}
\bar{\alpha}_C^i(\mathbf{q}) &= \frac{1}{T} \frac{\bar{A}_C^i(\mathbf{q}, \omega_q = 0; \omega_l)}{\omega_l} \bigg|_{i\omega_l \rightarrow \omega + i0}, \\
\bar{\sigma}_C^i(\mathbf{q}) &= \frac{\bar{S}_C^i(\mathbf{q}, \omega_q = 0; \omega_l)}{\omega_l} \bigg|_{i\omega_l \rightarrow \omega + i0}. \quad (\text{S.50})
\end{aligned}$$

Then, we obtain

$$\begin{aligned}
& \bar{\alpha}_C^a(\mathbf{q}) \\
&= C \cdot N(0)^2 W_0 \tau^2 q_z^2 \times \\
&\left[\frac{5\{\pi^2 u_{(1,0)}(t, \gamma) - 14\zeta(3)\gamma u_{(1,1)}(t, \gamma)\}}{96} \frac{v_F^2}{k_F^2 T} \right. \\
&\left. + \frac{\{-\pi^4 u_{(2,1)}(t, \gamma) + (-\psi^{(4)}(1/2)/6)\gamma u_{(2,2)}(t, \gamma)\}}{1920\pi^2} \frac{v_F^4}{T^3} \right], \quad (\text{S.51})
\end{aligned}$$

$$\begin{aligned}
& \bar{\alpha}_C^b(\mathbf{q}) \\
&= C \cdot N(0)^2 W_0 \tau^2 q_z^2 \\
&\left[\frac{5\{-\pi^2 u_{(1,0)}(t, \gamma) + \pi^2 \gamma w_{(1,1)}(t, \gamma)\}}{96} \frac{v_F^2}{k_F^2 T} \right. \\
&\left. + \frac{\{-2\pi^2 w_{(2,1)}(t, \gamma) + 2\pi^2 \gamma w_{(2,2)}(t, \gamma)\}}{1920\pi^2} \frac{v_F^4}{T^3} \right], \quad (\text{S.52})
\end{aligned}$$

$$\bar{\sigma}_C^a(\mathbf{q}) = C \cdot \frac{\pi^2 u_{(2,1)}(t, \gamma)}{192} \frac{v_F^3}{k_F T^2} N(0)^2 W_0 \tau^2 q_z^2, \quad (\text{S.53})$$

$$\bar{\sigma}_C^b(\mathbf{q}) = C \cdot \frac{w_{(2,1)}(t, \gamma)}{96} \frac{v_F^3}{k_F T^2} N(0)^2 W_0 \tau^2 q_z^2, \quad (\text{S.54})$$

where $t = 2\pi T/\Gamma$ and $\gamma = 1/2\pi\tau T$, and the definitions of dimensionless functions $u_{(i,j)}(t, \gamma)$ and $w_{(i,j)}(t, \gamma)$ are given in Sec. D. In clean limit ($\gamma \rightarrow 0$),

$$\begin{aligned}
& \bar{\alpha}_C^a(\mathbf{q}) \\
&= C \cdot N(0)^2 W_0 \tau^2 q_z^2 \times \\
&\left[\frac{5\pi^2 u_{(1,0)}(\frac{2\pi T}{\Gamma}, 0)}{96} \frac{v_F^2}{k_F^2 T} - \frac{\pi^2 u_{(2,1)}(\frac{2\pi T}{\Gamma}, 0)}{1920} \frac{v_F^4}{T^3} \right], \quad (\text{S.55})
\end{aligned}$$

$$\begin{aligned}
& \bar{\alpha}_C^b(\mathbf{q}) \\
&= C \cdot N(0)^2 W_0 \tau^2 q_z^2 \times \\
&\left[-\frac{5\pi^2 u_{(1,0)}(\frac{2\pi T}{\Gamma}, 0)}{96} \frac{v_F^2}{k_F^2 T} - \frac{w_{(2,1)}(\frac{2\pi T}{\Gamma}, 0)}{960} \frac{v_F^4}{T^3} \right], \quad (\text{S.56})
\end{aligned}$$

$$\begin{aligned}
& \bar{\sigma}_C^a(\mathbf{q}) \\
&= C \cdot \frac{\pi^2 u_{(2,1)}(\frac{2\pi T}{\Gamma}, 0)}{192} \frac{v_F^3}{k_F T^2} N(0)^2 W_0 \tau^2 q_z^2, \quad (\text{S.57})
\end{aligned}$$

$$\begin{aligned}
& \bar{\sigma}_C^b(\mathbf{q}) \\
&= C \cdot \frac{w_{(2,1)}(\frac{2\pi T}{\Gamma}, 0)}{96} \frac{v_F^3}{k_F T^2} N(0)^2 W_0 \tau^2 q_z^2. \quad (\text{S.58})
\end{aligned}$$

Finally, we complete the calculations of the Nernst and Hall conductivities, which are given by the integral over \mathbf{q} :

$$\alpha_{xy}^{Kubo} = \sum_{i=a,b,c} (-2eT) \sum_{\mathbf{q} C=\pm 1} \tilde{L}'_C(\mathbf{q}, \omega_q = 0; H) \bar{\alpha}_C^i(\mathbf{q}), \quad (\text{S.59})$$

$$\sigma_{xy} = \sum_{i=a,b,c} (2e^2 T) \sum_{\mathbf{q} C=\pm 1} \tilde{L}'_C(\mathbf{q}, \omega_q = 0; H) \bar{\sigma}_C^i(\mathbf{q}), \quad (\text{S.60})$$

where the chirality-dependent part of the BPS is given by

$$\tilde{L}'_C(\mathbf{q}, \omega_q; H) = C(5eH/4k_F^2 g) [L(\mathbf{q}, \omega_q)]^2. \quad (\text{S.61})$$

Using the expressions (S.55-S.58) and (S.71), we encounter ultraviolet divergence in the calculation of (S.59) and (S.60). Then, we introduce the cutoff momentum Λ . It is appropriate to set Λ as the same order as $1/\xi$, where ξ is the coherence length. The precise definition of ξ in this letter is given by Eq.(S.72) shown later. The reason is that the expansion of L^{-1} up to the second order of \mathbf{q} , (S.71), is justified when $|\mathbf{q}|$ is sufficiently smaller than

$1/\xi$, and, then, \tilde{L}'_C rapidly decreases as $|\mathbf{q}|$ increases in the region $|\mathbf{q}| > 1/\xi$, because of higher-order terms, as discussed in Sec. C. Besides, in $|\mathbf{q}| < \Lambda$, the expressions (S.55-S.58) are also justified, since $\xi k_F \gg 1$ is satisfied in almost all superconductors (indeed, $\xi k_F \sim 50$ in URu₂Si₂ [46]). To simplify the expressions of the final results, we assume that the domain of the integral is anisotropic: $\sum_i a_i q_i^2 \leq (a_x^2 a_z^3)^{1/5} \Lambda^2$, where the numerical factors are given by $a_x = a_y = 6/7$ and $a_z = 9/7$. Then, we obtain,

$$\begin{aligned} \alpha_{xy}^{Kubo \text{ chiral}} &= \frac{f\left(\frac{2\pi T}{\Gamma}\right)}{2304} \frac{\tau^2 e^2 W_0 v_F^4 \Lambda H}{\xi^4 g k_F^2 T^2} \\ &\times \left(1 - \frac{3\sqrt{\varepsilon} \arctan\left(\frac{\xi \Lambda}{\sqrt{\varepsilon}}\right)}{2\xi \Lambda} + \frac{1}{2 + 2(\xi \Lambda)^2/\varepsilon}\right), \end{aligned} \quad (\text{S.62})$$

$$\begin{aligned} \sigma_{xy}^{chiral} &= \frac{5f\left(\frac{2\pi T}{\Gamma}\right)}{1152} \frac{\tau^2 e^3 W_0 v_F^3 \Lambda}{\xi^4 g k_F^3 T} \\ &\times \left(1 - \frac{3\sqrt{\varepsilon} \arctan\left(\frac{\xi \Lambda}{\sqrt{\varepsilon}}\right)}{2\xi \Lambda} + \frac{1}{2 + 2(\xi \Lambda)^2/\varepsilon}\right), \end{aligned} \quad (\text{S.63})$$

in clean limit, where $\xi' = (a_x^2 a_z^3)^{1/10} \approx 1.05\xi$ and $f(t) = u_{(2,1)}(t, 0) + (2/\pi^2)w_{(2,1)}(t, 0)$. Since $\xi' \sim \xi$, we use ξ instead of ξ' in the following. For $T \sim T_c$, the above equations are reduced to Eqs. (4) and (5) in the main text.

C. Momentum Representation of Fluctuation Propagators under Zero Magnetic Field

In this section, we derive the expression of the fluctuation propagator of $d_{zx} \pm id_{zy}$ -wave superconductors under zero magnetic field, which is used in Sec. B. It is given by,

$$L^{-1}(\mathbf{q}, \omega_q) = -1/g + \Pi(\mathbf{q}, \omega_q), \quad (\text{S.64})$$

$$\Pi(\mathbf{q}, \omega_q) = T \sum_n \Pi_{\varepsilon_n}(\mathbf{q}, \omega_q), \quad (\text{S.65})$$

$$\begin{aligned} \Pi_{\varepsilon_n}(\mathbf{q}, \omega_q) &= \sum_{\mathbf{k}} |\phi(\mathbf{k})|^2 G\left(\mathbf{k} + \frac{\mathbf{q}}{2}, \varepsilon_{n+q}\right) G\left(-\mathbf{k} + \frac{\mathbf{q}}{2}, -\varepsilon_n\right), \end{aligned} \quad (\text{S.66})$$

where $G(\mathbf{k}, \varepsilon_k)^{-1} = i\tilde{\varepsilon}_k - \xi_{\mathbf{k}} = i(\varepsilon_k + \text{sgn}(\varepsilon_k)/2\tau) - \xi_{\mathbf{k}}$, $\phi(\mathbf{k}) = \sqrt{15/2}k_z(k_x + ik_y)/k_F^2$. Now, replacing the sum with the integral over the energy and average over the

Fermi surface, $\langle \dots \rangle_{\mathbf{k}}$, we obtain

$$\begin{aligned} \Pi_{\varepsilon_n}(\mathbf{q}, \omega_q) &= 2\pi N(0)\theta(\varepsilon_{n+q}\varepsilon_n) \left\langle \frac{|\phi(\mathbf{k})|^2}{|\tilde{\varepsilon}_{n+q} + \tilde{\varepsilon}_n| + i\Delta\xi(\mathbf{k}, \mathbf{q})} \right\rangle_{\mathbf{k}}, \end{aligned} \quad (\text{S.67})$$

where $N(0)$ is the density-of-state at the Fermi surface, θ is the Heaviside step function, and $\Delta\xi(\mathbf{k}, \mathbf{q}) = \xi_{\mathbf{k}+\mathbf{q}/2} - \xi_{\mathbf{k}-\mathbf{q}/2}$. Expanding it with respect to \mathbf{q} , we obtain the expression up to the quadratic term:

$$\begin{aligned} \Pi_{\varepsilon_n}(\mathbf{q}, \omega_q) &= \frac{2\pi N(0)\theta(\varepsilon_{n+q}\varepsilon_n)}{|\tilde{\varepsilon}_{n+q} + \tilde{\varepsilon}_n|} \times \\ &\left[\langle |\phi(\mathbf{k})|^2 \rangle_{\mathbf{k}} - \frac{\langle |\phi(\mathbf{k})|^2 (\mathbf{v}_{\mathbf{k}} \cdot \mathbf{q})^2 \rangle_{\mathbf{k}}}{|\tilde{\varepsilon}_{n+q} + \tilde{\varepsilon}_n|^2} \right] \\ &= \frac{2\pi N(0)\theta(\varepsilon_{n+q}\varepsilon_n)}{|\tilde{\varepsilon}_{n+q} + \tilde{\varepsilon}_n|} \left[1 - \frac{v_F^2 \sum_{i=x,y,z} a_i q_i^2}{|\tilde{\varepsilon}_{n+q} + \tilde{\varepsilon}_n|^2} \right], \end{aligned} \quad (\text{S.68})$$

where v_F is the Fermi velocity and $a_x = a_y = 6/7$ and $a_z = 9/7$ are numerical factors which reflect anisotropy of $V^\pm(\mathbf{k}, \mathbf{k}')$. Here, this expansion is justified when $\Delta\xi(\mathbf{k}, \mathbf{q})$ is sufficiently smaller than $|\tilde{\varepsilon}_{n+q} + \tilde{\varepsilon}_n|$. Due to the factor $\theta(\varepsilon_{n+q}\varepsilon_n)$, $|\tilde{\varepsilon}_{n+q} + \tilde{\varepsilon}_n|$ is equal to or larger than $2\pi T$, and, therefore, this condition is read as $v_F q \ll T \iff q \ll 1/\xi$, where the coherence length ξ used in this letter is precisely defined by Eq.(S.72).

Now, we take the sum over n , in which we introduce the cutoff energy ω_D for the pairing interaction and the upper limit of the frequency sum $N_{max} = \omega_D/2\pi T$ to remove the ultraviolet logarithmic divergence of the first sum:

$$\begin{aligned} \frac{\Pi(\mathbf{q}, \omega_q)}{N(0)} &= \psi\left(\frac{1}{2} + \frac{|\omega_q|}{4\pi T} + \frac{\omega_D}{2\pi T} + \frac{1}{4\pi T\tau}\right) \\ &- \psi\left(\frac{1}{2} + \frac{|\omega_q|}{4\pi T} + \frac{1}{4\pi T\tau}\right) \\ &+ \frac{v_F^2 a_i q_i^2}{2(4\pi T)^2} \psi''\left(\frac{1}{2} + \frac{1}{4\pi T\tau}\right). \end{aligned} \quad (\text{S.69})$$

The superconducting transition temperature T_c is defined by $L^{-1}(\mathbf{0}, 0)|_{T=T_c} = 0$, which is rewritten into

$$\psi\left(\frac{1}{2} + \frac{\omega_D}{2\pi T} + \frac{1}{4\pi T_c\tau}\right) - \psi\left(\frac{1}{2} + \frac{1}{4\pi T_c\tau}\right) = \frac{1}{gN(0)}. \quad (\text{S.70})$$

Therefore, we obtain the expression for the fluctuation propagator in the vicinity of T_c , i.e. $\varepsilon = \ln T/T_c \ll 1$:

$$\begin{aligned} L^{-1}(\mathbf{q}, \omega_q) &= -N(0) \left[\varepsilon + \psi\left(\frac{1}{2} + \frac{|\omega_q|}{4\pi T} + \frac{1}{4\pi T\tau}\right) \right. \\ &\left. - \psi\left(\frac{1}{2} + \frac{1}{4\pi T\tau}\right) + \sum_i \xi_i^2(\tau) q_i^2 \right], \end{aligned} \quad (\text{S.71})$$

where the coherence length is given by $\xi_i^2(\tau) = a_i \xi^2(\tau)$, where $\xi^2(\tau) = -v_F^2 \psi''(1/2 + 1/4\pi T\tau)/6(4\pi T)^2$. The coherence length used in this letter is defined by

$$\xi = \xi(\tau = \infty). \quad (\text{S.72})$$

Eq.(S.71) is the main result of this section.

D. Dimensionless Functions

In this section, we give the definitions of the dimensionless functions which appear in the formulae of the Nernst and Hall conductivities presented in the previous section. We also obtain their approximated but explicit expressions. The main result of this section is that the dimensionless function $f(t)$ which appears in Eqs.(4) and (5) in the main text is well approximated by a smooth function $\bar{f}^{app}(t)$ (S.89) for temperature regions where superconducting fluctuations are strong. We use it for the numerical calculation of temperature dependences of transport coefficients shown in FIG. 3 in the main text.

D1. Definitions

The definitions of dimensionless functions which appear in Eqs.(S.51)-(S.54) are

$$u_{(i,j)}(t, \gamma) = \frac{(-1)^{i+j+1}(i+j-1)!}{\psi^{(i+j)}(\frac{1}{2})} \left[\frac{2\pi T}{\omega_l} \times \sum_{0 \leq n, m \leq l-1} \frac{1}{(n+\frac{1}{2}+\frac{\gamma}{2})^i (m+\frac{1}{2}+\frac{\gamma}{2})^j (1+t|n-m|)} \right]_{\substack{i\omega_l \rightarrow \omega+i0, \\ \omega \rightarrow 0}}, \quad (\text{S.73})$$

$$w_{(i,j)}(t, \gamma) = \frac{(i-1)!(j-1)!}{(i+j-2)!\pi^2} \left[\frac{2\pi T}{\omega_l} \times \sum_{0 \leq n, m \leq l-1} \frac{1}{(n+\frac{1}{2}+\frac{\gamma}{2})^i (l-m-\frac{1}{2}+\frac{\gamma}{2})^j (1+t|n-m|)} \right]_{\substack{i\omega_l \rightarrow \omega+i0, \\ \omega \rightarrow 0}}, \quad (\text{S.74})$$

where (i, j) are nonnegative integers and the domains of definitions are $i+j \geq 1$ for $u_{(i,j)}(t)$, and $i, j \geq 1$ for $w_{(i,j)}(t, \gamma)$. An important property of these functions is that at $t = 0$,

$$u_{(i,j)}(t=0, \gamma) = w_{(i,j)}(t=0, \gamma) = 0. \quad (\text{S.75})$$

Also, their normalization factors are determined by the following conditions:

$$u_{(i,j)}(t=\infty, \gamma=0) = 1, \quad (\text{S.76})$$

$$w_{(i,j)}(t=\infty, \gamma) = \frac{1}{\gamma^{i+j-1}} + \mathcal{O}\left(\frac{1}{\gamma^{i+j-2}}\right) \text{ as } \gamma \rightarrow 0. \quad (\text{S.77})$$

Eqs. (S.75-S.77) are proved in Sec. D D3.

The dimensionless function $f(t)$ which appears in Eqs.(4) and (5) in the main text, and Eqs.(S.54) and (S.55) in Supplemental Material is defined by using $u_{(i,j)}(t, \gamma)$ and $w_{(i,j)}(t, \gamma)$ as,

$$f(t) = u_{(2,1)}(t, 0) + (2/\pi^2)w_{(2,1)}(t, 0)$$

D2. Approximation Functions

We, here, introduce analytically-solvable approximation functions for the dimensionless functions (S.73) and (S.74). They are defined by the analytic continuation of functions of the Matsubara frequencies:

$$u^{app}(t) = \frac{2\pi T}{\omega_l} \sum_{0 \leq n, m \leq l-1} \frac{1}{1+t|n-m|} \Bigg|_{\substack{i\omega_l \rightarrow \omega+i0, \\ \omega \rightarrow 0}}, \quad (\text{S.78})$$

$$w_{i+j}^{app}(t, \gamma) = \frac{2\pi T}{\omega_l} \sum_{0 \leq n, m \leq l-1} \frac{1}{(n-m+l+\gamma)^{i+j-1}} \frac{1}{1+t|n-m|} \Bigg|_{\substack{i\omega_l \rightarrow \omega+i0, \\ \omega \rightarrow 0}}, \quad (\text{S.79})$$

and they can be rewritten into compact expressions:

$$u^{app}(t) = -1 - \frac{2}{t} + \frac{2}{t^2} \psi' \left(\frac{1}{t} \right), \quad (\text{S.80})$$

$$w_{i+j}^{app}(t, \gamma) = \frac{(-1)^{i+j-2}}{(i+j-2)!} \frac{\partial^{i+j-2}}{\partial \gamma^{i+j-2}} w_2^{app}(t, \gamma),$$

$$w_2^{app}(t, \gamma) = \frac{1}{(1/t - \gamma)t} (\gamma \psi'(\gamma) - \frac{1}{t} \psi'(1/t)) - \frac{1}{(1/t + \gamma)t} (\gamma \psi'(1 + \gamma) - \frac{1}{t} \psi'(1/t)) - \frac{1}{\gamma}, \quad (\text{S.81})$$

which are derived in Sec. D D3.

We can expect that $u^{app}(t)$ and $w_{i+j}^{app}(t, \gamma)$ with small γ are good approximation functions for $u_{(i,j)}(t, \gamma=0)$ and $w_{(i,j)}(t, \gamma)$, respectively, because of the following reason. They have the same asymptotic behaviors as the original functions for $t \rightarrow \infty$, and also take the same values as the original ones at $t = 0$:

$$\frac{\partial^n u_{(i,j)}(t, \gamma=0)}{\partial t^n} \Bigg|_{t=\infty} = \frac{\partial^n u^{app}(t)}{\partial t^n} \Bigg|_{t=\infty}, \quad (\text{S.82})$$

$$u_{(i,j)}(t=0, \gamma) = u^{app}(t=0) = 0, \quad (\text{S.83})$$

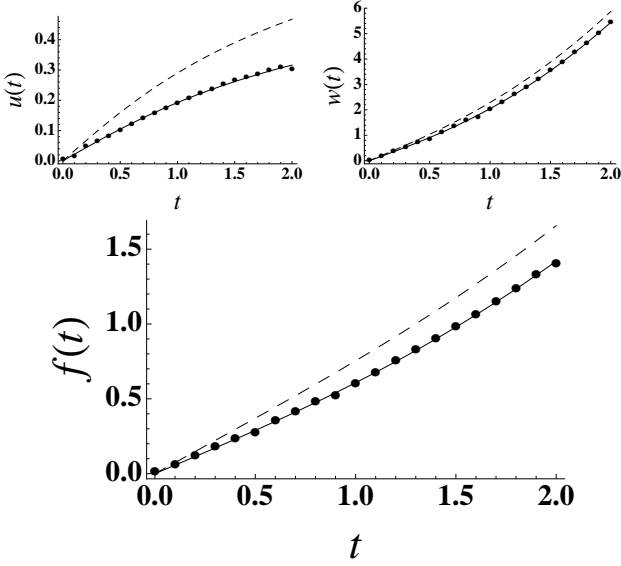


FIG. S.5: Upper Left (Upper Right, Lower): Numerical result for $u_{(2,1)}(t, 0)$ ($w_{(2,1)}(t, 0)$, $f(t)$) (dots), approximation function $u^{app}(t)$ ($w_3^{app}(t, 0)$, $f^{app}(t)$) (dashed line), and modified approximation function $\bar{u}^{app}(t)$ ($\bar{w}_3^{app}(t, 0)$, $\bar{f}^{app}(t)$) (solid line). The first and third ones coincide with each other quite well.

and

$$\begin{aligned} w_{(i,j)}(t = \infty, \gamma) &= w_{i+j}^{app}(t = \infty, \gamma) \\ &= \frac{1}{\gamma^{i+j-1}} + \mathcal{O}\left(\frac{1}{\gamma^{i+j-2}}\right) \quad \text{as } \gamma \rightarrow 0, \end{aligned} \quad (\text{S.84})$$

$$\begin{aligned} \left. \frac{\partial^n w_{(i,j)}(t, \gamma)}{\partial t^n} \right|_{\gamma: \text{fixed}, t=\infty} &= \left. \frac{\partial^n w_{i+j}^{app}(t, \gamma)}{\partial t^n} \right|_{\gamma: \text{fixed}, t=\infty} \\ &= 0, \quad \text{for } n \geq 1, \end{aligned} \quad (\text{S.85})$$

$$w_{(i,j)}(t = 0, \gamma) = w_{i+j}^{app}(t = 0, \gamma) = 0. \quad (\text{S.86})$$

We will prove these relations in Sec. D D3.

In FIG. S.5, we plot these approximation functions (dashed line) and numerical estimations of Eqs. (S.73) and (S.74) (dots) which are obtained by the Padé method. In this plot, we focus on $u_{(2,1)}(t, 0)$, $w_{(2,1)}(t, 0)$, and their sum, $f(t) = u_{(2,1)}(t, 0) + (2/\pi^2)w_{(2,1)}(t, 0)$, which appears in Eqs. (4) and (5). Here, the range of the plot is set to be $0 < t < 2.0$, which covers the region of superconducting fluctuations $t_c < t < xt_c$, $x \sim 3$, with $t_c = 2\pi T_c/\Gamma = 0.5$. In this calculations, we used the material parameters of URu₂Si₂, i.e. $T_c \sim 1.5\text{K}$ and $\Gamma \sim 1.5\text{meV}$ [16, 35]. As seen from FIG. S.5, the t -dependences of the approximation functions are qualitatively similar to the original functions. However, there are slight quantitative differences. Then, to improve the

approximation functions, we scale them as

$$\bar{u}^{app}(t) = c_u \cdot u^{app}(c'_u \cdot t), \quad (\text{S.87})$$

$$\bar{w}_3^{app}(t, 0) = c_w \cdot w_3^{app}(c'_w \cdot t, 0), \quad (\text{S.88})$$

$$\bar{f}^{app}(t) = \bar{u}^{app}(t) + \frac{2}{\pi^2} \bar{w}_3^{app}(t, 0), \quad (\text{S.89})$$

where the scaling parameter constants are obtained by fitting the numerical data, and we find $c_u = 0.72$, $c'_u = 0.91$, $c_w = 0.76$, and $c'_w = 1.14$. The improved approximation functions are also shown in FIG. S.5 (solid line) and we see that they coincide with the original functions quite well. Therefore, we use these smooth functions to calculate temperature dependences of transport coefficients in the main text.

D3. Proofs of Relations

In this subsection, we give proofs of relations used in the previous sections.

a. Proofs of Eq. (S.75)

We can easily verify the following relation,

$$\begin{aligned} u_{(i,j)}(t = 0, \gamma) &= c_{ij} \frac{2\pi T}{\omega_l} \sum_{0 \leq n, m \leq l-1} \frac{1}{(n + \frac{1}{2} + \frac{\gamma}{2})^2 (m + \frac{1}{2} + \frac{\gamma}{2})^2} \Bigg|_{\substack{i\omega_l \rightarrow \omega + i0, \\ \omega \rightarrow 0}} \\ &= c_{ij} \left[\frac{2\pi T}{\omega_l} \frac{\psi^{(i-1)}(\frac{1}{2}) - \psi^{(i-1)}(\frac{1}{2} + \frac{\omega_l}{2\pi T})}{(-1)^i (i-1)!} \right. \\ &\quad \times \left. \frac{\psi^{(i-1)}(\frac{1}{2}) - \psi^{(i-1)}(\frac{1}{2} + \frac{\omega_l}{2\pi T})}{(-1)^i (i-1)!} \right] \Bigg|_{\substack{i\omega_l \rightarrow \omega + i0, \\ \omega \rightarrow 0}} \\ &= 0 \end{aligned} \quad (\text{S.90})$$

where $c_{ij} = (-1)^{i+j+1} (i+j-1)! / \psi^{(i+j)}(\frac{1}{2})$. Similar calculation leads to $w_{(i,j)}(t, \gamma) = 0$. Then Eqs. (S.75) is proved.

b. Proofs of Eqs. (S.76) and (S.77)

First, we prove Eq. (S.76). Owing to the factor $1/(1+t|n-m|)$, only terms satisfying $n = m$ contribute to the sum at $t \rightarrow \infty$. Therefore,

$$\begin{aligned} u_{(i,j)}(t = \infty, \gamma = 0) &= c_{ij} \frac{2\pi T}{\omega_l} \sum_{n=0,1,\dots,l-1} \frac{1}{(n + \frac{1}{2})^{i+j}} \Bigg|_{\substack{i\omega_l \rightarrow \omega + i0, \\ \omega \rightarrow 0}} \\ &= c_{ij} \frac{2\pi T}{\omega_l} \frac{\psi^{(i+j-1)}(\frac{1}{2}) - \psi^{(i+j-1)}(\frac{1}{2} + \frac{\omega_l}{2\pi T})}{(-1)^{i+j} (i+j-1)!} \Bigg|_{\substack{i\omega_l \rightarrow \omega + i0, \\ \omega \rightarrow 0}} \\ &= c_{ij} / c_{ij} = 1. \end{aligned} \quad (\text{S.91})$$

Next, we prove Eq. (S.77). Taking the limit $t \rightarrow \infty$,

we have,

$$w_{(i,j)}(t = \infty, \gamma) = \frac{(i-1)!(j-1)!}{(i+j-2)!\pi^2} \times \frac{2\pi T}{\omega_l} \sum_{n=0,1,\dots,l-1} \frac{1}{(n+\frac{1}{2}+\frac{\gamma}{2})^i (l-n-\frac{1}{2}+\frac{\gamma}{2})^j} \Big|_{\substack{i\omega_l \rightarrow \omega+i0, \\ \omega \rightarrow 0}}. \quad (\text{S.92})$$

Now, let

$$\begin{aligned} \tilde{w}_{(i,j)}(\gamma) &= \frac{2\pi T}{\omega_l} \sum_{n=0,1,\dots,l-1} \frac{1}{(n+\frac{1}{2}+\frac{\gamma}{2})^i (l-n-\frac{1}{2}+\frac{\gamma}{2})^j} \Big|_{\substack{i\omega_l \rightarrow \omega+i0, \\ \omega \rightarrow 0}}. \end{aligned} \quad (\text{S.93})$$

Then,

$$\begin{aligned} \tilde{w}_{(i,j)}(\gamma) &= \frac{1}{\gamma} (\tilde{w}_{(i,j-1)}(\gamma) + \tilde{w}_{(i-1,j)}(\gamma)) \\ &= \frac{1}{\gamma^2} (\tilde{w}_{(i,j-2)}(\gamma) + 2\tilde{w}_{(i-1,j-1)}(\gamma) + \tilde{w}_{(i-2,j)}(\gamma)) \\ &\vdots \\ &= \frac{(i+j-2)!}{(i-1)!(j-1)!} \frac{1}{\gamma^{i+j-1}} (\tilde{w}_{(1,0)}(\gamma) + \tilde{w}_{(0,1)}(\gamma)) \\ &\quad + c'_1 \frac{1}{\gamma^{i+j-2}} (\tilde{w}_{(2,0)}(\gamma) + \tilde{w}_{(0,2)}(\gamma)) \\ &\quad + c'_2 \frac{1}{\gamma^{i+j-3}} (\tilde{w}_{(3,0)}(\gamma) + \tilde{w}_{(0,3)}(\gamma)) \\ &\quad + \dots \end{aligned} \quad (\text{S.94})$$

where c'_1, c'_2, \dots are constants. By using

$$\begin{aligned} \tilde{w}_{(i,0)}(\gamma = 0) &= \frac{2\pi T}{\omega_l} \sum_{n=0,1,\dots,l-1} \frac{1}{(n+\frac{1}{2})^i} \Big|_{\substack{i\omega_l \rightarrow \omega+i0, \\ \omega \rightarrow 0}} \\ &= \frac{(-1)^{i+1} \psi^{(i)}(\frac{1}{2})}{(i-1)!}, \end{aligned} \quad (\text{S.95})$$

we obtain

$$\begin{aligned} w_{(i,j)}(t = \infty, \gamma) &= \frac{(i-1)!(j-1)!}{(i+j-2)!\pi^2} \tilde{w}_{(i,j)}(\gamma) \\ &= \frac{1}{\gamma^{i+j-1}} + \mathcal{O}\left(\frac{1}{\gamma^{i+j-2}}\right) \quad \text{as } \gamma \rightarrow 0. \end{aligned} \quad (\text{S.96})$$

Then, the normalization conditions (S.76) and (S.77) are proved.

c. Proofs of Eqs. (S.80) and (S.81)

Now, introducing $N = n-m$ and dividing the region of summation in (S.78) into $\sum_{n \leq m} + \sum_{n \geq m} - \sum_{n=m}$, we obtain,

$$\begin{aligned} u^{app}(t) &= 2 \times \left[\frac{2\pi T}{\omega_l} \sum_{N=0,1,\dots,l-1} \frac{l-N}{1+tN} \right] \Big|_{\substack{i\omega_l \rightarrow \omega+i0, \\ \omega \rightarrow 0}} - 1 \\ &= -1 - \frac{2}{t} + \frac{2}{t^2} \left[\frac{2\pi T}{\omega_l} \sum_{N=0,1,\dots,l-1} \frac{1}{N+1/t} \right] \Big|_{\substack{i\omega_l \rightarrow \omega+i0, \\ \omega \rightarrow 0}} \\ &\quad + \frac{2}{t} \left[\sum_{N=0,1,\dots,l-1} \frac{1}{1+tN} \right] \Big|_{\substack{i\omega_l \rightarrow \omega+i0, \\ \omega \rightarrow 0}} \\ &= -1 - \frac{2}{t} + \frac{2}{t^2} \psi' \left(\frac{1}{t} \right). \end{aligned} \quad (\text{S.97})$$

From it we can derive Eq. (S.80). Furthermore, Eq. (S.81) can be obtain by similar calculations.

d. Proofs of Eqs. (S.82) and (S.83)

First, we prove Eq. (S.82). The $n = 0$ case immediately follows from Eq. (S.76) and the explicit expression for $u^{app}(t)$, (S.80). For $n \geq 1$,

$$\begin{aligned} \frac{\partial^n u_{(i,j)}(t, \gamma = 0)}{\partial t^n} \Big|_{t=\infty} &= c_{ij} \frac{2\pi T}{\omega_l} \sum_{0 \leq a, b \leq l-1} d_{ij}^{ab} (-1)^n n! \frac{|a-b|^n}{(1+t|a-b|)^{n+1}} \Big|_{\substack{i\omega_l \rightarrow \omega+i0, \\ \omega \rightarrow 0}}, \end{aligned} \quad (\text{S.98})$$

where $d_{ij}^{ab} = 1/(a+\frac{1}{2})^i (b+\frac{1}{2})^j$. Now, owing to the factor $1/(1+t|a-b|)^{n+1}$, the contributions from the terms satisfying $a \neq b$ become zero in $t \rightarrow \infty$ limit. Moreover, the other terms, which satisfy $a = b$, are also zero for $n \geq 1$ on account of the factor $|a-b|^n$. Therefore, we find that Eq. (S.98) is zero in $t \rightarrow \infty$ limit. A similar calculation leads $\partial^n u^{app}(t)/\partial t^n|_{t=\infty} = 0$, which also directly follows from the explicit expression (S.80). Then, Eq. (S.82) for any $n \geq 0$ is proven.

On the other hand, Eq. (S.83) instantly follows from Eq. (S.75) and a calculation similar to Eq. (S.90).

e. Proofs of Eqs. (S.84), (S.85), and (S.86)

The equivalence between the LHS and RHS of Eq. (S.84) has been already proven (S.77). Then, we now prove the equivalence between the middle one and the RHS. Owing to the factor $1/(1+t|n-m|)$, only terms

satisfying $n = m$ contribute to the sum at $t \rightarrow \infty$:

$$\begin{aligned}
w_{i+j}^{app}(t = \infty, \gamma) &= \frac{2\pi T}{\omega_l} \sum_{n=0,1,\dots,l-1} \frac{1}{(l+\gamma)^{i+j-1}} \bigg|_{i\omega_l \rightarrow \omega + i0, \omega \rightarrow 0} \\
&= \frac{1}{\gamma^{i+j-1}}.
\end{aligned} \tag{S.99}$$

Then, the whole of Eq. (S.84) is proven.

On the other hand, Eqs. (S.85) and (S.86) can be derived with techniques similar to those used in the derivations of Eq (S.82) for $n \geq 1$ and Eq. (S.83).

E. Magnetization

In this section we discuss the magnetization and derive Eqs. (7) and (8). In this letter \hat{A} means an matrix whose element is $A(\mathbf{x}, \mathbf{y})$ and $\hat{1}_{\mathbf{x}, \mathbf{y}} = \delta(\mathbf{x} - \mathbf{y})$. The free energy in the presence of the magnetic field, $\mathbf{H} = (0, 0, H)$, is given by

$$\begin{aligned}
F[H] &= T \sum_{\omega_q, C=\pm 1} \text{Trln}(-\hat{L}_C^{-1}(\omega_q; H)) \\
&= 2T \sum_{\omega_q} \text{Trln}(\hat{1} - ge^{-2i\hat{\Phi}}\hat{\Pi}(\omega_q; H)) \\
&+ T \sum_{\omega_q} \text{Trln} \left[\hat{1} - \left(\frac{5eHg}{4k_F^2} \right)^2 \frac{e^{-2i\hat{\Phi}}\hat{\Pi}'^2(\omega_q; H)}{(1 - ge^{-2i\hat{\Phi}}\hat{\Pi}(\omega_q; H))^2} \right].
\end{aligned} \tag{S.100}$$

Then, the magnetic susceptibility is given as

$$\chi = \chi_{dia} + \chi_{chiral}, \tag{S.101}$$

where

$$\begin{aligned}
\chi_{dia} &= - \frac{\partial^2}{\partial H^2} \left\{ 2T \sum_{\omega_q} \text{Trln}(\hat{1} - ge^{-2i\hat{\Phi}}\hat{\Pi}(\omega_q; H)) \right\} \bigg|_{H \rightarrow 0} \\
&\tag{S.102}
\end{aligned}$$

is the fluctuation diamagnetism term which appears also in non-chiral superconductors [37], where the factor 2 reflects the fact that the number of fluctuation channel

is two, and

$$\begin{aligned}
\chi_{chiral} &= - \frac{\partial^2}{\partial H^2} \left\{ T \sum_{\omega_q} \text{Trln} \left[\hat{1} - \frac{\left(\frac{5eHg}{4k_F^2} \right)^2 e^{-2i\hat{\Phi}}\hat{\Pi}'^2(\omega_q; H)}{\left(\hat{1} - ge^{-2i\hat{\Phi}}\hat{\Pi}(\omega_q; H) \right)^2} \right] \right\} \bigg|_{H \rightarrow 0} \\
&= 2T \left(\frac{5eg}{4k_F^2} \right)^2 \sum_{\omega_q} \text{Tr} \left[\frac{\hat{\Pi}'^2(\omega_q; H=0)}{\left(\hat{1} - g\hat{\Pi}(\omega_q; H=0) \right)^2} \right]
\end{aligned} \tag{S.103}$$

is the contribution unique to chiral superconductors. Now, we evaluate the chirality-induced term (S.103). Neglecting the $\omega_q \neq 0$ terms, which are less singular in the vicinity of T_c than the $\omega_q = 0$ one, we obtain

$$\chi_{chiral} = \frac{25e^2 T}{64\pi k_F^4 \varepsilon^3 (N(0)g)^2 \varepsilon^{1/2}} > 0, \tag{S.104}$$

which is positive, indicating the paramagnetic response due to MC-coupling. In this calculation, we used the momentum representation of the BPS, (S.71).

F. Dependence of the Results on Specific Form of W , Dimensionality, and Pairing Symmetry

In this section, we discuss to what extent the main results, (4) and (5), depend on the functional form of the remonetized four-point vertex, $W(\mathbf{k}, \omega_k)$, the spatial dimensionality, and the pairing symmetry of chiral superconducting states.

Here, we summarize the main results of this section: 1) The result that $\alpha_{xy}^{Kubo, chiral}$ and σ_{xy}^{chiral} are proportional to τ^2 is not changed by these three conditions. 2) The critical behavior may be changed by the dimensionality and the pairing symmetry, but not by the functional form of $W(\mathbf{k}, \omega_k)$. 3) The magnitudes of $\alpha_{xy}^{Kubo, chiral}$ and σ_{xy}^{chiral} depend on the specific form of $W(\mathbf{k}, \omega_k)$: they are decreased as the momentum-dependence is stronger.

In the succeeding subsections, we will discuss the details.

F1. τ -Dependence

Irrespective of functional forms of $W(\mathbf{k}, \omega_k)$, spatial dimensionality, and the pairing symmetry of chiral superconducting states, $\bar{A}_C^{(i)}(\mathbf{q}, \omega_q; \omega_l)$ and $\bar{S}_C^{(i)}(\mathbf{q}, \omega_q; \omega_l)$ ($i = a, b$) always have terms with the factor $(i\omega_l + 1/\tau)^{-2}$ (and $(i\omega_l + 1/\tau)^{-1}$ when $i = c$), as shown in Sec. F F4. Moreover, in any case of chiral fluctuations, the expression for the chirality-dependent fluctuation propagator, (S.17), holds besides numerical factors. Therefore, it is

general that $\alpha_{xy\text{chiral}}^{Kubo}$ and $\sigma_{xy\text{chiral}}$ are proportional to τ^2 in clean limit. However, their magnitudes depend on the functional form of W as discussed in Sec. F F3

F2. Critical Behavior

We discuss how the critical exponents of $\alpha_{xy\text{chiral}}^{Kubo}$ and $\sigma_{xy\text{chiral}}$ as functions of $\varepsilon = \log T/T_c$ depend on the functional form of $W(\mathbf{k}, \omega_k)$, the dimensionality, and the pairing symmetry of chiral superconducting states.

As mentioned above, we can use the expression of the chirality-dependent fluctuation propagator, (S.17) generally except numerical factors. Then, from Eq. (S.59), we obtain

$$\alpha_{xy\text{chiral}}^{Kubo} \text{ or } \sigma_{xy\text{chiral}} \propto \int d^d \mathbf{q} \frac{q^\Delta}{(\xi^2 q^2 + \varepsilon)^2} \quad (\text{S.105})$$

in the vicinity of the T_c , where Δ is defined by $\bar{A}_C(\mathbf{q}, \omega_q = 0; \omega_l)$ or $\bar{S}_C(\mathbf{q}, \omega_q = 0; \omega_l) = \mathcal{O}(q^\Delta)$, as $q \rightarrow 0$. Therefore we find that the spatial dimensionality and Δ determine the critical exponent.

As will be shown in Sec F F4, Δ does not depend on specific forms of $W(\mathbf{k}, \omega_k)$, but is affected by the spatial dimensionality and pairing symmetries of chiral superconducting states. Therefore, the critical exponents of (4) and (5) are independent of the specific form of $W(\mathbf{k}, \omega_k)$, though the dimensionality may change them.

In TABLE S.1, we present the exponents for some typical examples. In the case of three dimensional chiral $d_{zx} \pm id_{zy}$ superconducting fluctuation, $\Delta = 2$, (see Eqs (S.44-S.47)), and then the critical behavior is, $\alpha_{xy\text{chiral}}^{Kubo} \propto \text{const} - \sqrt{\varepsilon}$ (see (4)). Moreover, in the case of two-dimensional chiral- p one (the d -vector is given by $\mathbf{d}(\mathbf{k}) = (0, 0, k_x \pm ik_y)$, and then $\phi(\mathbf{k}) \propto (k_x \pm ik_y)$), which is believed to be the pairing symmetry of Sr_2RuO_4 [15], we find, from straightforward calculations, $\bar{A}_C, \bar{S}_C \propto q^0$ and then $\alpha_{xy\text{chiral}}^{Kubo}, \sigma_{xy\text{chiral}} \propto 1/\varepsilon$, where the critical behavior of the former (latter) is the same as (less singular than) that of the conventional AL term in two spatial dimensions [30].

	Δ	
	0	2
2D	$1/\varepsilon$	$\log \varepsilon$
	(Sr ₂ RuO ₄)	
3D	$1/\sqrt{\varepsilon}$	$\text{const} - \sqrt{\varepsilon}$
	(URu ₂ Si ₂)	

TABLE S.1: Critical behaviors of $\alpha_{xy\text{chiral}}^{Kubo}$ and $\sigma_{xy\text{chiral}}$, which is decided by the dimensionality and the pairing symmetry of chiral superconducting states.

F3. Specific Form of W

In this subsection, we discuss how the magnitudes of $\alpha_{xy\text{chiral}}^{Kubo}$ and $\sigma_{xy\text{chiral}}$ are influenced by the momentum-dependence of W .

Here we consider the case of arbitrary chiral pairing symmetry that is given by $\phi(\mathbf{p}) \propto Y_l^m(\hat{p})$ (three dimension) or $\propto e^{im\theta_{\mathbf{p}}}$ (two dimension), where Y_l^m is the spherical harmonic function and $\theta_{\mathbf{p}}$ is the angle defined by $\tan \theta_{\mathbf{p}} = p_x/p_y$. As discussed in Sec. B, only the odd parts of \bar{A}_C or \bar{S}_C with respect to time reversal, $C \rightarrow -C$, give nonzero contributions. The integrands of $\bar{A}_{C=1}^{(i)} - \bar{A}_{C=-1}^{(i)}$ and $\bar{S}_{C=1}^{(i)} - \bar{S}_{C=-1}^{(i)}$ generally ($i = a, b, c$) contain the factor (see FIG. S.4):

$$\begin{aligned} & \phi^\dagger(\mathbf{p})\phi(\mathbf{p}')W(\mathbf{p} - \mathbf{p}', \omega_k) - (\phi \leftrightarrow \phi') \\ & \propto \sin(m\theta)W(\mathbf{p} - \mathbf{p}', \omega_k), \end{aligned} \quad (\text{S.106})$$

where θ is the angle between \mathbf{p}_\parallel and \mathbf{p}'_\parallel . Here, \mathbf{p}_\parallel represents the projection of the vector \mathbf{p} onto the ab -plane. The relation between these vectors and angle is drawn in FIG. S.6. From this equation, we find that, due to the factor $\sin(m\theta)$, the magnitudes of $\alpha_{xy\text{chiral}}^{Kubo}$ and $\sigma_{xy\text{chiral}}$ are large in the case that the magnitude of $W(\mathbf{p} - \mathbf{p}', \omega_k)$ is large for $\theta \sim (\text{half odd integer}) \times (\pi/m)$.

We, now, consider a simple case that the momentum dependence of $W(\mathbf{k}, \omega_k)$ has a dominant peak at $\mathbf{k} = \mathbf{Q}_0$ with width $1/\xi_{\mathbf{Q}_0}$. When the peak is sharp, the domain of integration that contributes to $\alpha_{xy\text{chiral}}^{Kubo}$ and $\sigma_{xy\text{chiral}}$ is restricted to the region in which $\mathbf{p} - \mathbf{p}' \sim \mathbf{Q}_0$. However, it is quite exceptional that the angle θ is nearly equal to $(\text{half odd integer}) \times (\pi/m)$ when \mathbf{p} and \mathbf{p}' satisfy the above condition. Therefore, generally, the magnitudes of $\alpha_{xy\text{chiral}}^{Kubo}$ and $\sigma_{xy\text{chiral}}$ are small when $\xi_{\mathbf{Q}_0}$ is large. On the other hand, when $\xi_{\mathbf{Q}_0}$ is small, the domain of integration in which $\theta \sim (\text{half odd integer}) \times (\pi/m)$, is included in the domain in which $W(\mathbf{p} - \mathbf{p}', \omega_k)$ has large values, and then the magnitudes of $\alpha_{xy\text{chiral}}^{Kubo}$ and $\sigma_{xy\text{chiral}}$ are larger than the case of large $\xi_{\mathbf{Q}_0}$. As a result, the magnitudes of $\alpha_{xy\text{chiral}}^{Kubo}$ and $\sigma_{xy\text{chiral}}$ increase as $\xi_{\mathbf{Q}_0}$ become smaller.

Finally, we consider the case of URu₂Si₂. In this case, the pairing function is given by $\phi(\mathbf{p}) \propto Y_2^1(\hat{p})$ and the interaction is mediated via short-range antiferromagnetic spin-fluctuation with $\mathbf{Q}_0 = (0, 0, 2\pi/a_z^{\text{lattice}})$, where a_z^{lattice} is the lattice constant. Here $\xi_{\mathbf{Q}_0}$ is the correlation length of this fluctuation. Since θ is zero when $\mathbf{Q}_0 = \mathbf{p} - \mathbf{p}'$, then, the magnitudes of $\alpha_{xy\text{chiral}}^{Kubo}$ and $\sigma_{xy\text{chiral}}$ become small, if this fluctuation were to be long-range.

F4. Auxiliary Explanations

a. Factors $(i\omega_l + 1/\tau)^{-2}$ and $(i\omega_l + 1/\tau)^{-1}$ in $\bar{A}_C^{(i)}(\mathbf{q}, \omega_q; \omega_l)$ and $\bar{S}_C^{(i)}(\mathbf{q}, \omega_q; \omega_l)$

Here, we show that in any case of the functional form of W , the dimensionality, and the pairing symme-

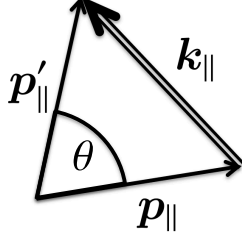


FIG. S.6: Relation between the relative momenta of fluctuating Cooper pairs, \mathbf{p} , \mathbf{p}' , the momentum of four-point vertex, \mathbf{k} , and the angle θ that is the angle between \mathbf{p}_{\parallel} and \mathbf{p}'_{\parallel} . Here, \mathbf{p}_{\parallel} represents the components parallel to ab -plane.

try of chiral superconducting states, $\bar{A}_C^i(\mathbf{q}, \omega_q; \omega_l)$ and $\bar{S}_C^i(\mathbf{q}, \omega_q; \omega_l)$ for $i = a, b$ always have the terms proportional to $(i\omega_l + 1/\tau)^{-2}$ (and $(i\omega_l + 1/\tau)^{-1}$ for $i = c$).

First, for $i = a$, in any case, we can write (see FIG. S.4 (a)):

$$\begin{aligned} & \bar{A}_C^a(\mathbf{q}, \omega_q; \omega_l) \text{ or } \bar{S}_C^a(\mathbf{q}, \omega_q; \omega_l) \\ &= \sum_{\mathbf{p}, \mathbf{s}, \mathbf{q}, n, m} G(\mathbf{p}, \varepsilon_{n-l}) G(\mathbf{p}, \varepsilon_n) G(\mathbf{s}, \varepsilon_{m-l}) G(\mathbf{s}, \varepsilon_m) \\ & \quad \times g^a(\mathbf{p}, \mathbf{s}, n, m; l), \end{aligned} \quad (\text{S.107})$$

where g^a is a certain function. Then, integrating it over the energy $\xi_{\mathbf{p}}$ along the contour shown in FIG. S.7 (a), we obtain the factor $(i\varepsilon_n - i\varepsilon_{n-l})^{-1} = (i\omega_l + 1/\tau)^{-1}$ at $n = 0, 1, \dots, l-1$, and this factor does not appear for other values of m . Similarly, the integration over $\xi_{\mathbf{s}}$ also generates the factor $(i\omega_l + 1/\tau)^{-1}$ at $m = 0, 1, \dots, l-1$. Therefore, $\bar{A}_C^a(\mathbf{q}, \omega_q; \omega_l)$ and $\bar{S}_C^a(\mathbf{q}, \omega_q; \omega_l)$ have terms with factor $(i\omega_l + 1/\tau)^{-2}$. We can prove this relation also for the case of $i = b$ by using a similar argument.

Next, for $i = c$, we can write (see FIG. S.4 (c)-1):

$$\begin{aligned} & \bar{A}_C^c(\mathbf{q}, \omega_q; \omega_l) \text{ or } \bar{S}_C^c(\mathbf{q}, \omega_q; \omega_l) \\ &= \sum_{\mathbf{s}, \mathbf{p}, m, n} G(\mathbf{s}, \varepsilon_{m+l}) G(\mathbf{s}, \varepsilon_m) \\ & \quad \times G(\mathbf{q} - \mathbf{s}, -\varepsilon_{m-q}) G(\mathbf{q} - \mathbf{s}, -\varepsilon_{m-q+l}) \\ & \quad \times G(\mathbf{q} - \mathbf{p}, -\varepsilon_{n-q+l}) G(\mathbf{p}, \varepsilon_{n+l}) \\ & \quad \times g^c(\mathbf{s}, \mathbf{p}, \mathbf{q}, m; l), \end{aligned} \quad (\text{S.108})$$

where g^c is a certain function. When $\max\{-l, q-l\} \leq m \leq \min\{-1, q-1\}$, the pole structure of the complex $\xi_{\mathbf{s}}$ -plane is given by FIG. S.7 (c), and then the integrating over $\xi_{\mathbf{s}}$ generates the terms proportional to $(i\omega_l + 1/\tau)^{-1}$. Such terms appear also for the value of m , at which three poles exist in the upper-half plane or lower-half-plane and the other one exists in the other side (FIG. S.7 (c)-2), and do not appear when all poles exist on the same side. On the other hand, integrating over $\xi_{\mathbf{p}}$ generates no term proportional to $(i\omega_l + 1/\tau)^{-1}$. Therefore, $\bar{A}_C^c(\mathbf{q}, \omega_q; \omega_l)$ and $\bar{S}_C^c(\mathbf{q}, \omega_q; \omega_l)$ have terms with a factor $(i\omega_l + 1/\tau)^{-1}$.

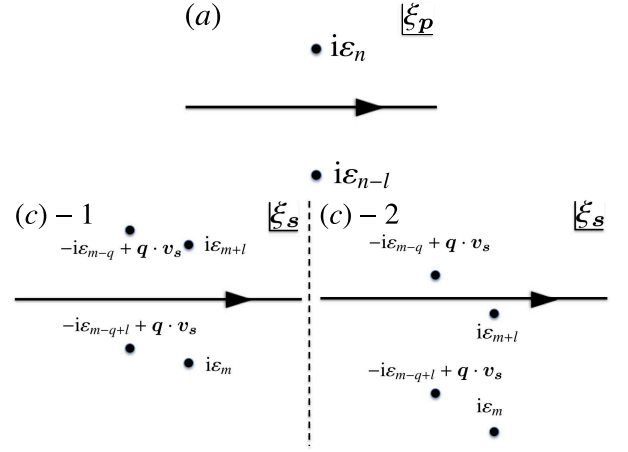


FIG. S.7: The contours of energy-integration in Eqs. (S.107) (upper panel) and (S.108) (lower panels). Dots represent poles of order 1. Each contour integration generates the factor $(i\omega_l + 1/\tau)^{-1}$.

b. Critical exponent Δ independent of specific form of W

In this subsection, we show that the critical exponent Δ is independent of the specific form of $W(\mathbf{k}, \omega_k)$. We consider the case that the interaction is repulsive, i.e. $W(\mathbf{k}, \omega_k) > 0$.

For every $i = a, b, c$, we can write \bar{A}_C^i or \bar{S}_C^i as

$$\begin{aligned} & \bar{A}_C^i(\mathbf{q}, \omega_q = 0; \omega_l) \text{ or } \bar{S}_C^i(\mathbf{q}, \omega_q = 0; \omega_l) \\ &= \sum_{\mathbf{k}, \omega_k} h(\mathbf{q}, \mathbf{k}, \omega_k; \omega_l) W(\mathbf{k}, \omega_k). \end{aligned} \quad (\text{S.109})$$

The important point is that W is independent of \mathbf{q} . Then, expanding $h(\mathbf{q}, \mathbf{k}, \omega_k; \omega_l)$ with respect to \mathbf{q} , we obtain

$$\begin{aligned} & \bar{A}_C^i(\mathbf{q}, \omega_q = 0; \omega_l) \text{ or } \bar{S}_C^i(\mathbf{q}, \omega_q = 0; \omega_l) \\ &= \sum_{\mathbf{k}, \omega_k} h(\mathbf{k}, \omega_k; \omega_l) W(\mathbf{k}, \omega_k) \\ & \quad + q_x^2 \sum_{\mathbf{k}, \omega_k} h_{xx}(\mathbf{k}, \omega_k; \omega_l) W(\mathbf{k}, \omega_k) \\ & \quad + q_y^2 \sum_{\mathbf{k}, \omega_k} h_{yy}(\mathbf{k}, \omega_k; \omega_l) W(\mathbf{k}, \omega_k) \\ & \quad + \dots \end{aligned} \quad (\text{S.110})$$

Here, we neglect terms that vanish after performing the integration, (S.105). Δ is the lowest number of dimensions with respect to \mathbf{q} of the term in which $\sum h_* W$ is nonzero, for $*$ = , $xx, yy, zz, xxxx, xxyy, \dots$. Since W is positive definite, $\sum h_* W$ leads to $\sum h_* W' = 0$, where W' is another form of potential energy that is positive definite. Therefore, Δ for some particular form of W is the same as that of another one, W' , and thus, we conclude that Δ is independent of the specific form of W .